

# Defective lymphoid organogenesis underlies the immune deficiency caused by a heterozygous S32I mutation in I $\kappa$ B $\alpha$

Jana L. Mooster,<sup>1,3</sup> Severine Le Bras,<sup>1,3</sup> Michel J. Massaad,<sup>1,3</sup> Haifa Jabara,<sup>1,3</sup> Juhan Yoon,<sup>1,3</sup> Claire Galand,<sup>1,3</sup> Balthasar A. Heesters,<sup>2,6</sup> Oliver T. Burton,<sup>1,3</sup> Hamid Mattoo,<sup>7</sup> John Manis,<sup>4,5</sup> and Raif S. Geha<sup>1,3</sup>

<sup>1</sup>Division of Allergy and Immunology and <sup>2</sup>Program in Cellular and Molecular Medicine, Boston Children's Hospital, Boston, MA 02115

<sup>3</sup>Department of Pediatrics, <sup>4</sup>Division of Transfusion Medicine, and <sup>5</sup>Department of Pathology, Harvard Medical School, Boston, MA 02115

<sup>6</sup>Department of Medical Microbiology, University Medical Center Utrecht, 3584 CX Utrecht, Netherlands

<sup>7</sup>Center for Cancer Research, Massachusetts General Hospital, Boston, MA 02114

**Patients with ectodermal dysplasia with immunodeficiency (ED-ID) caused by mutations in the inhibitor of NF- $\kappa$ B  $\alpha$  (I $\kappa$ B $\alpha$ ) are susceptible to severe recurrent infections, despite normal T and B cell numbers and intact in vitro lymphocyte function. Moreover, the outcome of hematopoietic stem cell transplantation (HSCT) in these patients is poor despite good engraftment. Mice heterozygous for the I $\kappa$ B $\alpha$  S32I mutation found in patients exhibited typical features of ED-ID. Strikingly, the mice lacked lymph nodes, Peyer's patches, splenic marginal zones, and follicular dendritic cells and failed to develop contact hypersensitivity (CHS) or form germinal centers (GCs), all features not previously recognized in patients and typical of defective noncanonical NF- $\kappa$ B signaling. Lymphotoxin  $\beta$  receptor (LT $\beta$ R)-driven induction of chemokines and adhesion molecules mediated by both canonical and noncanonical NF- $\kappa$ B pathways was impaired, and levels of p100 were markedly diminished in the mutant. I $\kappa$ B $\alpha$  mutant  $\rightarrow$  Rag2<sup>-/-</sup>, but not WT  $\rightarrow$  I $\kappa$ B $\alpha$  mutant, bone marrow chimeras formed proper lymphoid organs and developed CHS and GCs. Defective architectural cell function explains the immunodeficiency and poor outcome of HSCT in patients with I $\kappa$ B $\alpha$  deficiency and suggests that correction of this niche is critical for reconstituting their immune function.**

## CORRESPONDENCE

Raif S. Geha:  
Raif.Geha@childrens.harvard.edu

Abbreviations used: AD, autosomal dominant; BAFF, B cell activating factor; CBC, complete blood count; CHS, contact hypersensitivity; EDA, ectodysplasin A; ED-ID, ectodermal dysplasia with immunodeficiency; ES, embryonic stem; FDC, follicular DC; GC, germinal center; HSCT, hematopoietic stem cell transplantation; I $\kappa$ B, inhibitor of NF- $\kappa$ B; IKK, I $\kappa$ B kinase; LTi, lymphoid tissue inducer; MZ, marginal zone; NEMO, NF- $\kappa$ B essential modulator; NIK, NF- $\kappa$ B-inducing kinase; OXA, oxazolone; PP, Peyer's patch; PNA, peanut agglutinin; qPCR, quantitative PCR; TD, T dependent; TI, T independent.

Innate and adaptive immune responses depend on the activation of NF- $\kappa$ B, which has five family members: RelA (p65), RelB, c-Rel, NF- $\kappa$ B1 (p50), and NF- $\kappa$ B2 (p52; Hayden and Ghosh, 2008, 2012; Napetschnig and Wu, 2013). NF- $\kappa$ B dimers are retained in the cytoplasm by inhibitors of NF- $\kappa$ B (I $\kappa$ Bs), mainly I $\kappa$ B $\alpha$  in immune cells, which prevent the nuclear translocation of NF- $\kappa$ B. In the canonical NF- $\kappa$ B pathway, used by TLRs, CD40, and receptors for antigen, IL-1, TNF, and ectodysplasin A (EDA), receptor ligation causes activation of the I $\kappa$ B kinase (IKK) complex, which consists of the NF- $\kappa$ B essential modulator (NEMO/IKK $\gamma$ ) and the catalytic subunits IKK $\alpha$  and IKK $\beta$  (Bonizzi and Karin, 2004). The activated IKK complex phosphorylates I $\kappa$ B $\alpha$  at Ser 32 and Ser 36, which targets it for polyubiquitination and degradation

by the 26S proteasome (Karin and Ben-Neriah, 2000). The released NF- $\kappa$ B dimers (primarily p50/p65) translocate to the nucleus and activate transcription of genes encoding inflammatory cytokines, chemokines, adhesion molecules, and I $\kappa$ B $\alpha$  itself (Hayden et al., 2006; Hayden and Ghosh, 2008). In the noncanonical pathway, used by lymphotoxin  $\beta$  receptor (LT $\beta$ R), B cell activating factor receptor (BAFF-R), and CD40, NF- $\kappa$ B-inducing kinase (NIK) activates IKK $\alpha$ , resulting in the phosphorylation of p100 (NF- $\kappa$ B2), which is in complex with RelB in the cytoplasm. p100 then undergoes

© 2015 Mooster et al. This article is distributed under the terms of an Attribution-Noncommercial-Share Alike-No Mirror Sites license for the first six months after the publication date (see <http://www.rupress.org/terms>). After six months it is available under a Creative Commons License (Attribution-Noncommercial-Share Alike 3.0 Unported license, as described at <http://creativecommons.org/licenses/by-nc-sa/3.0/>).

polyubiquitination and proteasome processing into p52, allowing the p52:RelB dimer to translocate into the nucleus and activate the transcription of genes involved in lymphoid organogenesis (Dejardin et al., 2002; Seymour et al., 2006). There is cross talk between the canonical and noncanonical NF- $\kappa$ B pathways. NIK-dependent activation of IKK $\alpha$  can cause I $\kappa$ B $\alpha$  phosphorylation and degradation, p50:p65 regulates the expression of p100 and RelB, and p100 regulates RelA/p65-containing complexes (Matsushima et al., 2001; Tucker et al., 2007; Shih et al., 2011; Chen et al., 2013).

Ectodermal dysplasia with immunodeficiency (ED-ID) is characterized by sparse hair, conical teeth, reduced number of sweat glands, and susceptibility to severe infections (Kere et al., 1996; Srivastava et al., 2001; Orange and Geha, 2003; Picard et al., 2011). The X-linked form of ED-ID is caused by hypomorphic mutations in NEMO (Puel et al., 2004; Hanson et al., 2008). Autosomal-dominant (AD) ED-ID is caused by heterozygous hypermorphic mutations in the I $\kappa$ B $\alpha$  gene *NFKB1A* (Courtois et al., 2003; Kawai et al., 2012). Six mutations in I $\kappa$ B $\alpha$ , S32I, W11X, E14X, Q9X, M37K, and S36Y, have been identified in AD ED-ID (Courtois et al., 2003; Janssen et al., 2004; McDonald et al., 2007; Lopez-Granados et al., 2008; Ohnishi et al., 2012; Schimke et al., 2013; Yoshioka et al., 2013). In each case, the mutation impairs phosphorylation-driven degradation of the mutant protein, resulting in the sequestration of NF- $\kappa$ B in the cytoplasm (Courtois et al., 2003; McDonald et al., 2007; Kawai et al., 2012). In both forms of ED-ID, activation of the canonical NF- $\kappa$ B pathway is impaired, resulting in ED caused by defective signaling downstream of the EDA receptor, impaired TLR responses, and decreased in vitro B cell response to CD40 ligation (Orange et al., 2005). The severity of the disease correlates with the degree of NF- $\kappa$ B impairment (Orange and Geha, 2003).

Two aspects of the disease phenotype of patients affected by I $\kappa$ B $\alpha$  deficiency have long been a puzzle. The patients suffer from severe, recurrent, and potentially fatal infections despite having normal or elevated T and B cell numbers and intact in vitro T cell function (Courtois et al., 2003; Janssen et al., 2004; McDonald et al., 2007; Kawai et al., 2012). The outcome of hematopoietic stem cell transplantation (HSCT) in these patients is poor in spite of good engraftment of donor lymphoid cells. Of three patients treated with HSCT, only one with the S32I I $\kappa$ B $\alpha$  mutation has survived, but continues to suffer from recurrent infections despite excellent donor lymphoid cell engraftment (Dupuis-Girod et al., 2006; Cancrini, C., personal communication). We have created an I $\kappa$ B $\alpha$  S32I knock-in mouse model of AD ED-ID to gain insights into the disease. The I $\kappa$ B $\alpha$  mutant mouse recapitulates many of the ectodermal and immune abnormalities found in patients with ED-ID. Strikingly, the mutant completely lacked LNs and Peyer's patches (PPs), and its spleen lacked follicles, marginal zones (MZs), MZ B cells, and follicular DCs (FDCs) and failed to form germinal centers (GCs), all features not previously recognized in patients with ED-ID and typical of defective noncanonical NF- $\kappa$ B signaling. The levels of p100 and noncanonical NF- $\kappa$ B signaling in response to LT $\beta$ R ligation

were decreased in the I $\kappa$ B $\alpha$  mutant. Analysis of BM radiation chimeras demonstrated that the defective lymphoid organogenesis in the I $\kappa$ B $\alpha$  mutant is caused by a defect in nonhematopoietic cells, thus explaining the poor outcome of HSCT in patients with I $\kappa$ B $\alpha$  deficiency.

## RESULTS

### Mice heterozygous for the S32I mutation in I $\kappa$ B $\alpha$ have ED and impaired I $\kappa$ B $\alpha$ phosphorylation and degradation

The strategy for the generation and identification of the heterozygous I $\kappa$ B $\alpha$  S32I mutant (I $\kappa$ B $\alpha$  mutant) mice is shown in Fig. S1. I $\kappa$ B $\alpha$  mutant mice were born at the normal Mendelian ratio but were significantly smaller in size and weight than their WT littermates (Fig. 1, A and B) and had a 50% survival rate at 8 wk compared with 100% for WT littermates (Fig. 1 C). I $\kappa$ B $\alpha$  mutant mice are missing their third molars, lack guard hairs, and have hypoplastic eccrine glands (Fig. 1, D–F), a phenotype observed in mice with disruption of the *Eda* gene, mutated in patients with X-linked anhidrotic ED (Srivastava et al., 2001).

Immunoblotting cannot distinguish between WT I $\kappa$ B $\alpha$  and the S32I mutant proteins. We sought evidence for the expression of the mutant protein in heterozygous I $\kappa$ B $\alpha$  mutant mice by examining the susceptibility of I $\kappa$ B $\alpha$  to phosphorylation and degradation after stimulation of fibroblasts with IL-1 $\beta$ . I $\kappa$ B $\alpha$  phosphorylation was significantly weaker in fibroblasts from mutant mice compared with WT littermates (Fig. 1 G). I $\kappa$ B $\alpha$  was mostly degraded by 15 min and completely degraded by 30 min in WT fibroblasts. In contrast, there was markedly less I $\kappa$ B $\alpha$  degradation in the mutant fibroblasts. Similar results were obtained when the fibroblasts were stimulated with TNF and LPS, two other well-known activators of the canonical NF- $\kappa$ B pathway (not depicted).

BMDCs were differentiated from BM cells with GM-CSF and IL-4 and used to examine the response to TLR ligation in a homogeneous population of cells. BMDCs from I $\kappa$ B $\alpha$  mutant mice secreted significantly less TNF in response to TLR1/2, TLR4, TLR7, and TLR9 ligands (Fig. 1 H). Furthermore, up-regulation of *Vcam1* (*Vascular adhesion molecule 1*) and *Icam1* (*Intercellular adhesion molecule 1*) gene expression and of VCAM1 surface expression after TNF stimulation, which are dependent on canonical NF- $\kappa$ B signaling (Dejardin et al., 2002; Winning et al., 2010), was deficient in MEFs from I $\kappa$ B $\alpha$  mutant mice (Fig. 1, I and J). Collectively, these results indicate that the I $\kappa$ B $\alpha$  mutant mice we generated represent a faithful model of ED-ID caused by heterozygous I $\kappa$ B $\alpha$  S32I mutation.

### Defective secondary lymphoid organogenesis in I $\kappa$ B $\alpha$ mutant mice

The gross appearance, weight, and cellularity of the thymus and the distribution of thymocyte subsets into CD4<sup>-</sup>CD8<sup>-</sup> double-negative cells, CD4<sup>+</sup>CD8<sup>+</sup> double-positive cells, and CD4<sup>+</sup> or CD8<sup>+</sup> single-positive cells were comparable in I $\kappa$ B $\alpha$  mutant mice and WT littermates (not depicted). BM cellularity and distribution of (B220<sup>+</sup>IgM<sup>-</sup>CD43<sup>+</sup>) pro-B, (B220<sup>+</sup>IgM<sup>-</sup>CD43<sup>-</sup>) pre-B, (B220<sup>+</sup>IgM<sup>+</sup>) immature, and

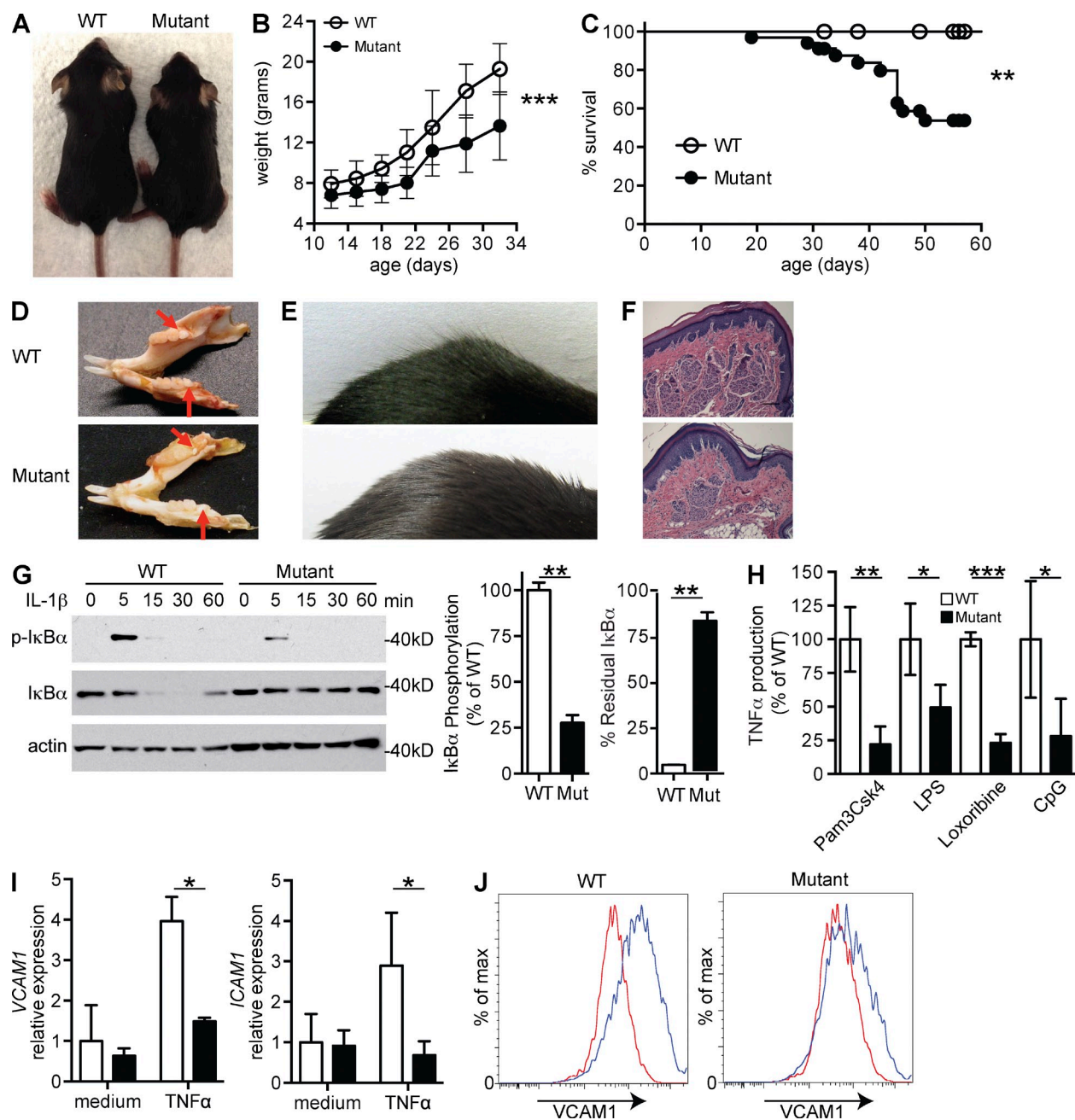


**Figure 1.  $I\kappa B\alpha$  mutant mice have ED, impaired  $I\kappa B\alpha$  processing, and deficient TLR response.** (A)  $I\kappa B\alpha$  mutant mouse and WT littermate photographed at 3 wk of age. Data are representative of >20 mice per group. (B and C) Growth (B) and Kaplan-Meier survival (C) curves of  $I\kappa B\alpha$  mutant mice and WT littermates weighed every 3–4 d and observed daily. Data were derived from 34 mutant mice and 19 WT littermates weighed. (D–F) Photographs of mandibular bones (D) and fur (E) and H&E staining of footpad sections (F) in 6 wk-old  $I\kappa B\alpha$  mutant mouse and WT littermate. Red arrows in D show the missing third molars in the mutant mice. Data are representative of four or more mice per group in three independent experiments. Bar, 100  $\mu$ m. (G) Immunoblot of fibroblast lysates using antibodies to phospho- $I\kappa B\alpha$  or  $I\kappa B\alpha$ . Actin was used as a loading control. Pooled results of  $I\kappa B\alpha$  phosphorylation at 5 min using three mice per group in three independent experiments. (H) TNF as measured by ELISA in supernatants of BMDCs stimulated with the TLR ligands PamCsk4 (TLR1/2), LPS (TLR4), loxoribine (TLR7), and CpG oligonucleotide (TLR9). Data are representative of four mice per group in two independent experiments for PamCsk4 and LPS and four mice per group in three independent experiments for loxoribine and CpG. (I and J) qPCR analysis of *Vcam1* and *Icam1* mRNA (I) and flow cytometric analysis of VCAM1 surface expression (J) after TNF stimulation in MEFs from  $I\kappa B\alpha$  mutant mice and WT controls. Results in I are expressed relative to unstimulated WT MEFs. Data are representative of three mice per group in three independent experiments. Circles and columns represent means, and bars represent SD in B, C, and G–I. \*,  $P < 0.05$ ; \*\*,  $P < 0.01$ ; \*\*\*,  $P < 0.001$ .

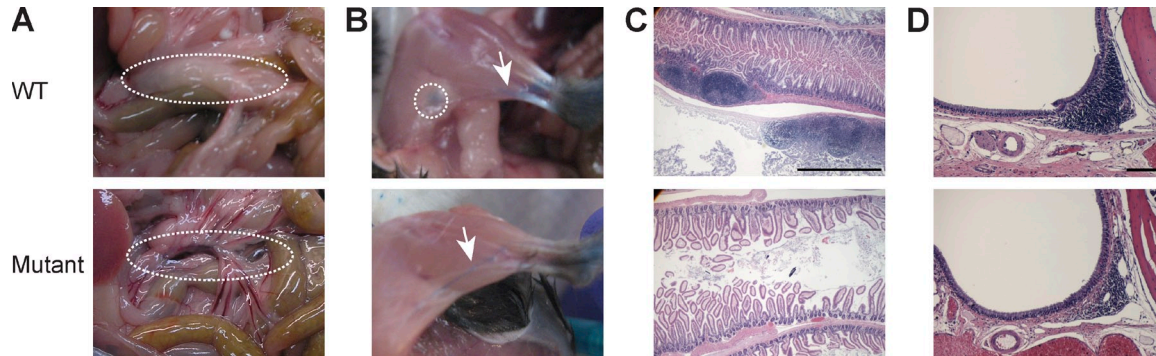


**Figure 2.**  $\text{I}\kappa\text{B}\alpha$  mutant mice lack LNs and PPs. (A and B) Photograph of mesenteric area (A) and popliteal LNs (B) in an  $\text{I}\kappa\text{B}\alpha$  mutant mouse and WT littermate. Mice in B were injected with Evan's blue. The normal position of LNs is outlined by a dotted circle. Arrows indicate the lymphatic vessels. (C and D) Longitudinal sections of the small intestine (C) and transverse sections of the head at the level of the nasal cavities (D) were stained with H&E. Bars, 1,000  $\mu\text{m}$ . Data in A–D are representative of a minimum of three mice per group in three independent experiments.

( $\text{B220}^{2+}\text{IgM}^{+}$ ) mature B cell subsets were comparable in  $\text{I}\kappa\text{B}\alpha$  mutant mice and WT littermates (not depicted).

Gross examination revealed no visible cervical, axillary, inguinal, or mesenteric LNs in >15  $\text{I}\kappa\text{B}\alpha$  mutant mice examined (Fig. 2 A and not depicted). No LN tissue could be detected in hematoxylin and eosin (H&E)-stained serial sections of the inguinal fat pad in  $\text{I}\kappa\text{B}\alpha$  mutant mice (not depicted). To confirm the absence of LNs, we injected mice in the footpad with Evan's blue dye. Blue-colored lymphatic vessels were readily apparent in both mutant and WT mice. Blue-colored LNs could be detected in the popliteal, inguinal, and paraaortic area in WT mice, but were absent in the mutants (Fig. 2 B and not depicted). Examination of H&E-stained sections of the small intestine revealed no detectable PPs in seven mutant mice compared with  $7.1 \pm 2.3$  PPs in seven WT littermates examined (Fig. 2 C). However, nasal-associated lymphoid tissue (NALT) was present in  $\text{I}\kappa\text{B}\alpha$  mutant mice, although it was less abundant than in WT mice (Fig. 2 D). The numbers of circulating lymphocytes were significantly increased in the  $\text{I}\kappa\text{B}\alpha$  mutant mice (Fig. 3 A), a finding also reported in patients with the S32I  $\text{I}\kappa\text{B}\alpha$  mutation (Courtois et al., 2003; Janssen et al., 2004) and in  $\text{LT}\alpha^{-/-}$ ,  $\text{LT}\beta^{-/-}$ , and  $\text{LT}\beta\text{R}^{-/-}$  mice that lack both LNs and PPs but have detectable NALT (De Togni et al., 1994; Ware et al., 1995; Alimzhanov et al., 1997; Matsumoto et al., 1997; Fütterer et al., 1998; Tumanov et al., 2003).

The cellularity of the spleen was greater in  $\text{I}\kappa\text{B}\alpha$  mutant mice than WT littermates, but the difference was not statistically significant (Fig. 3 B). The number of splenic T cells and the distribution of  $\text{CD4}^{+}$  and  $\text{CD8}^{+}$  subsets were comparable between the  $\text{I}\kappa\text{B}\alpha$  mutant mice and WT littermates (Fig. 3 C). Analysis of B cell subsets revealed comparable percentages of  $\text{B220}^{+}\text{CD93}^{+}$  transitional B cells and  $\text{B220}^{+}\text{CD23}^{+}\text{CD21}^{-}$  follicular cells in the two groups but drastically reduced percentages of  $\text{B220}^{+}\text{CD23}^{-}\text{CD21}^{+}$  MZ B cells in mutant spleens (Fig. 3, D and F). The percentages of MZ B cells in the blood were comparable in the mutant and WT littermates ( $12.1 \pm 1.0\%$  in the mutant vs.  $10.6 \pm 1.8\%$  in WT littermates;  $n = 3$ ). Given the severe decrease in splenic MZ B cells in the mutant, this result suggests a retention defect but does

not rule out a defect in development of MZ cells.  $\text{I}\kappa\text{B}\alpha$  mutant mice had increased numbers of  $\text{CD11b}^{+}\text{F4/80}^{+}$  macrophages but normal numbers of  $\text{CD11b}^{+}\text{Ly6G}^{+}$  granulocytes and  $\text{CD3}^{-}\text{NK1.1}^{+}$  cells and  $\text{CD11c}^{+}$  DCs compared with WT littermates (not depicted). The percentages of  $\text{CD11c}^{+}\text{MHCII}^{+}\text{B220}^{+}$  plasmacytoid DCs and  $\text{CD11c}^{+}\text{MHCII}^{+}\text{CD11b}^{+}\text{CD4}^{+}$  and  $\text{CD11c}^{+}\text{MHCII}^{+}\text{CD11b}^{+}\text{CD8}^{-}\text{CD4}^{-}$  myeloid DCs were comparable between the two groups, whereas the percentage of  $\text{CD11c}^{+}\text{MHCII}^{+}\text{CD11b}^{-}\text{CD8}^{+}$  lymphoid DCs was significantly reduced in the mutant ( $9.3 \pm 0.9\%$  in the mutant vs.  $14.8 \pm 1.0\%$  in WT littermates;  $n = 3$ ;  $P < 0.05$ ).

$\text{I}\kappa\text{B}\alpha$  mutant mice had a severely disorganized splenic architecture. H&E staining revealed virtual absence of follicles (Fig. 3 G). Immunofluorescence analysis revealed that  $\text{MOMA}^{+}$  macrophages were present in  $\text{I}\kappa\text{B}\alpha$  mutant mice but failed to form the ring structure typical of a MZ (Fig. 3 H). The number of  $\text{Madc1}^{+}$  cells, which represent the endothelial cells that line the marginal sinus, was decreased, and the organization of these cells was disrupted in the  $\text{I}\kappa\text{B}\alpha$  mutant (Fig. 3 I).  $\text{FDCM1}^{+}$  FDCs were absent from the spleens of the mutant (Fig. 3 J).

#### Normal number of lymphoid tissue inducer (LTi) cells but defective response to $\text{LT}\beta\text{R}$ ligation and TNF in the $\text{I}\kappa\text{B}\alpha$ mutant

Lymphorganogenesis is initiated in the embryo by the interaction of LTi cells with stromal organizer cells, which express  $\text{LT}\beta\text{R}$  (Rennert et al., 1996; Mebius, 2003; Bénézech et al., 2010). FACS analysis of intestine from embryonic day (E) 17 embryos revealed the presence of higher percentages and numbers of  $\text{CD45}^{+}\text{CD3}^{-}\text{CD4}^{+}\text{IL-7R}^{+}$  LTi cells in  $\text{I}\kappa\text{B}\alpha$  mutant mice compared with WT littermates (Fig. 4, A and B), indicating that the  $\text{I}\kappa\text{B}\alpha$  mutation did not interfere with the development of LTi cells.

LTi cells express the  $\text{LT}\beta\text{R}$  ligand  $\text{LT}\alpha_{1}\beta_{2}$ , whereas stromal cells express  $\text{LT}\beta\text{R}$ .  $\text{LT}\beta\text{R}$  signaling in stromal cells is essential for lymphoid organogenesis (Fu and Chaplin, 1999). Both the canonical and noncanonical  $\text{NF-}\kappa\text{B}$  pathways are

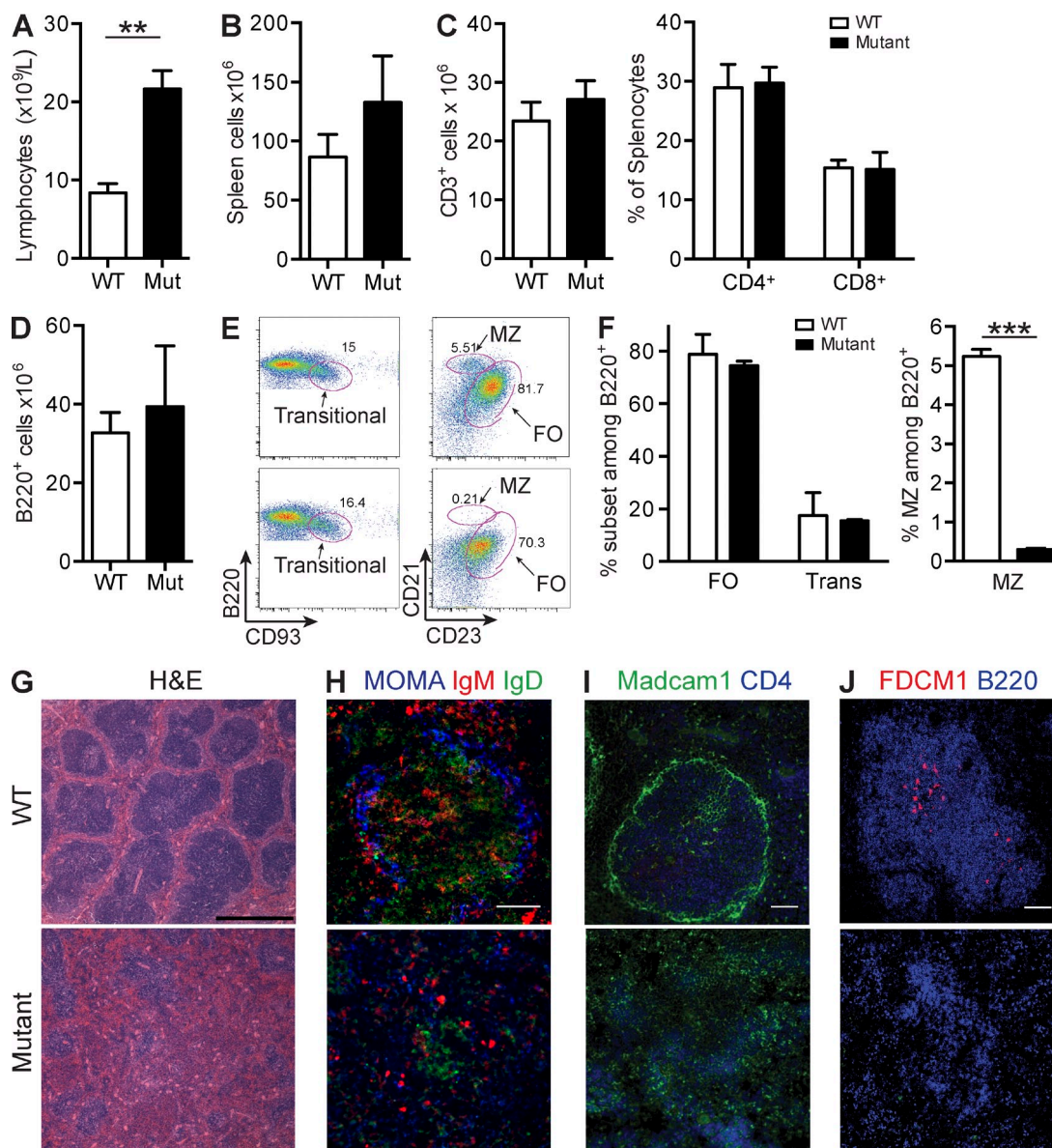


**Figure 3.  $\text{I}\kappa\text{B}\alpha$  mutant mice lack splenic follicles, MZs, MZ B cells, and FDCs.** (A) Blood lymphocyte numbers in  $\text{I}\kappa\text{B}\alpha$  mutant mice and WT littermates evaluated by CBC analysis using HEMAVET 950FS. Data are representative of three mice per group in two independent experiments. (B–D) Numbers of total splenocytes (B),  $\text{CD}3^+$ ,  $\text{CD}4^+$ , and  $\text{CD}8^+$  T cells (C), and  $\text{B}220^+$  B cells (D) in  $\text{I}\kappa\text{B}\alpha$  mutant mice and WT littermates calculated by multiplying the spleen cell counts evaluated in a hemocytometer by the percentage of lymphocytes and those of  $\text{CD}3^+$ ,  $\text{CD}4^+$ , and  $\text{CD}8^+$  T cells and of  $\text{B}220^+$  obtained by flow cytometry. Data are representative of three to eight mice per group in three independent experiments. (E and F) Distribution of  $\text{CD}93^+$  transitional (Trans) B cells,  $\text{CD}21^- \text{CD}23^+$  follicular (FO) B cells, and  $\text{CD}21^+ \text{CD}23^-$  MZ B cells in gated  $\text{B}220^+$  splenic B cells (E) and percentages of these cells among splenic  $\text{B}220^+$  cells (F) in  $\text{I}\kappa\text{B}\alpha$  mutant mice and WT littermates analyzed by flow cytometry. Data are representative of three to six mice per group in three independent experiments. (G–J) Sections of naive spleens stained with H&E (G) and the presence of cell staining for MOMA, IgM, and IgD (H), Madcam1 and CD4 (I), and FDCM1 and B220 (J) as determined by immunofluorescence. Bars: (G) 500  $\mu\text{m}$ ; (H–J) 100  $\mu\text{m}$ . Data in G–J is representative of a minimum of four mice per group in three independent experiments. Columns and bars represent mean and SD. \*\*,  $P < 0.01$ ; \*\*\*,  $P < 0.001$ .

activated by  $\text{LT}\beta\text{R}$  and are important for the expression of adhesion molecules and chemokines that drive lymphoid organogenesis, with the noncanonical pathway playing a major role (Miyawaki et al., 1994; Koike et al., 1996; Shinkura et al., 1999; Dejardin et al., 2002; Lo et al., 2006; Vondenhoff et al., 2009). The absence of secondary lymphoid structures in  $\text{I}\kappa\text{B}\alpha$  mutant mice prompted us to examine  $\text{LT}\beta\text{R}$  signaling in

these mice. We stimulated MEFs, as surrogates for stromal cells, with the agonistic  $\text{LT}\beta\text{R}$  mAb AFH6 and examined the induction of *Vcam1* and *Icam1* expression, as readouts of canonical NF- $\kappa\text{B}$  activation (Dejardin et al., 2002), *Cxcl10* (*C-X-C motif chemokine 10*) expression, as a readout of predominantly canonical NF- $\kappa\text{B}$  activation (Hoffmann et al., 2003; Caposio et al., 2007; Shultz et al., 2009), and *Madcam1*

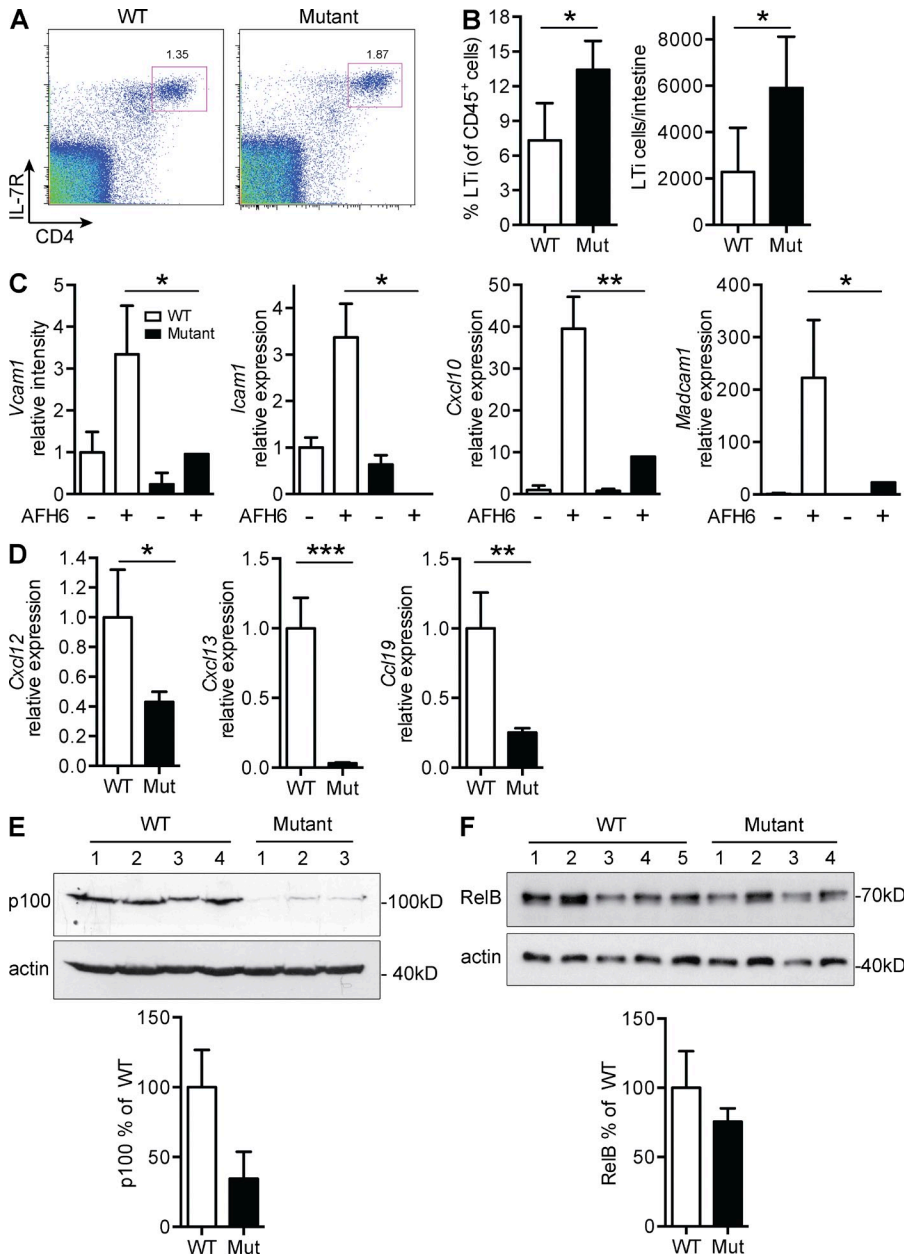


**Figure 4. Defective response to LTβR ligation and decreased p100 levels in the IκBα mutant.** (A) CD4<sup>+</sup>IL-7R<sup>+</sup> LTI cells in CD45<sup>+</sup>CD3<sup>-</sup> gated intestinal cells of E17 embryos analyzed by flow cytometry. (B) Percentage of LTI cells among CD45<sup>+</sup>CD3<sup>-</sup> cells analyzed by flow cytometry and numbers of LTI cells in E17 intestinal cells calculated from the numbers of CD45<sup>+</sup>CD3<sup>-</sup> cells and percentage of LTI cells. Data in A and B are representative of five mice per group. (C) *Vcam1*, *Icam1*, *Cxcl10*, and *Madcam1* mRNA expression in MEFs stimulated with the LTβR mAb AHF6 and analyzed by qPCR. Results are expressed as fold increase relative to unstimulated WT controls. Data are representative of three mice per group in three experiments. (D) *Cxcl12*, *Cxcl13*, and *Ccl19* mRNA expression in the spleen of IκBα mutant and WT littermates analyzed by qPCR. Results are expressed as fold increase relative to WT controls. Data are representative of four mice per group in two experiments. (E and F) Representative immunoblot analysis of p100 (E) and RelB (F) in lysates of purified splenic B cells with actin as control (top) and p100 (E) and RelB (F) expression in B cells from the IκBα mutant relative to WT (bottom) calculated at the ratio of p100 and RelB to actin in lysates of B cells from the IκBα mutant relative to that in lysates of WT B cells. Data are representative of three to seven mice per group in three experiments. Columns and lines represent means, and bars represent SD in B-F. \*, P < 0.05; \*\*, P < 0.01; \*\*\*, P < 0.001.

expression, as a readout of noncanonical NF-κB pathway activation downstream of LTβR (Ganef et al., 2011). Expression of all these genes after stimulation with LTβR mAb AFH6 was significantly reduced in MEFs from IκBα mutant mice compared with WT controls (Fig. 4 C and not depicted).

Induction of the chemokine genes *Ccl19* (*C-C motif chemokine 19*), *Cxcl12*, and *Cxcl13* after LTβR signaling is important for lymphoid organogenesis and is dependent on the noncanonical NF-κB pathway (van de Pavert et al., 2009; van de Pavert and Mebius, 2010). Because LTβR failed to up-regulate the expression of these genes in WT MEFs (not depicted), we examined their baseline expression in the spleen. Expression of all three chemokine genes was significantly

reduced in spleens of IκBα mutant mice compared with WT littermates (Fig. 4 D).

Expression in cell lines of the genes that encode for the noncanonical NF-κB family members p100 and RelB have been reported to be regulated by the canonical NF-κB pathway (Liptay et al., 1994; Bren et al., 2001). The level of p100, but not RelB, was significantly reduced in B cells from IκBα mutant mice (Fig. 4, E and F). NIK levels were comparable in B cells from IκBα mutant mice and WT controls (not depicted). These findings suggest that the S32I IκBα mutation impairs signaling via the noncanonical NF-κB pathway because it results in diminished expression of p100.

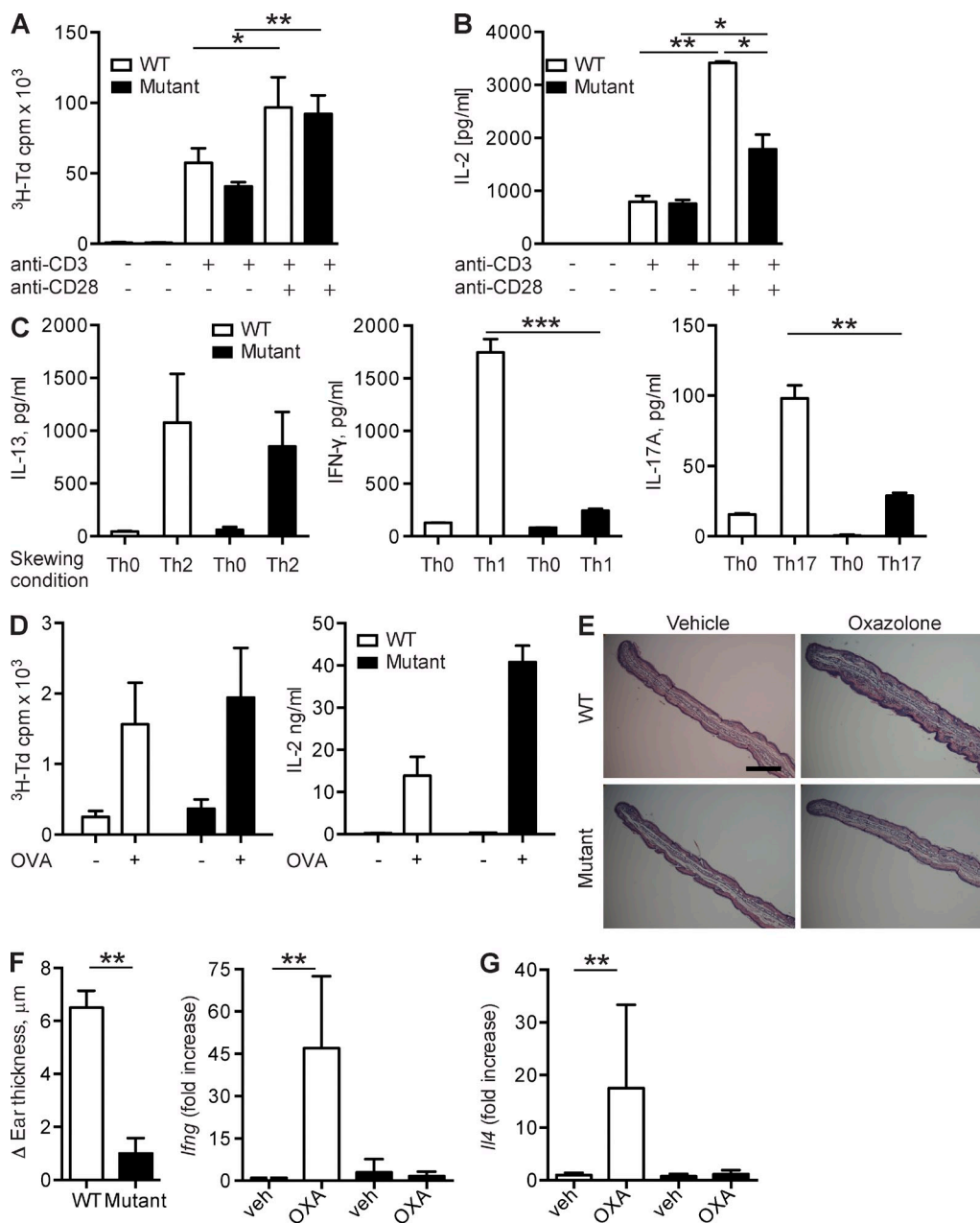


**Figure 5. Normal intrinsic T cell function but impaired CHS in  $I\kappa B\alpha$  mutant mice.** (A and B) Proliferation determined by [<sup>3</sup>H]thymidine incorporation into DNA (A) and IL-2 secretion determined by ELISA of supernatants (B) by purified splenic T cells stimulated for 3 (A) or 2 (B) d with immobilized anti-CD3 mAb (A) or immobilized anti-CD3 + soluble anti-CD28 mAb (B). Data represent a minimum of five mice per group in A and four in B in three independent experiments. (C) Cytokine secretion determined by ELISA on supernatants of purified splenic T cells stimulated with immobilized anti-CD3 mAb + anti-CD28 mAbs in the absence of added cytokines (Th0 condition) or in Th2, Th1, or Th17 polarizing conditions. Data represent five mice per group in three independent experiments. (D) Proliferation determined by [<sup>3</sup>H]thymidine incorporation into DNA and IL-2 production determined by ELISA of supernatants by splenocytes from i.p. immunized mice stimulated with OVA for 3 d for proliferation and 2 d for IL-2 production. Data represent five mice per group in three independent experiments. (E–G) H&E-stained sections of the ears (E), increase in ear thickness measured by a micrometer (F), and *Irf4* and *Il-4* mRNA expression determined by qPCR (G) 24 h after ear challenge with OXA or vehicle. Results in F are represented as the fold increase relative to vehicle-challenged ears of WT controls. Bar, 200 μm. Data in E–G represent five to seven mice per group in three independent experiments. Columns and bars in A–D, F, and G represent mean and SD. \*,  $P < 0.05$ ; \*\*,  $P < 0.01$ ; \*\*\*,  $P < 0.001$ .

#### Normal intrinsic T cell function but impaired delayed contact hypersensitivity (CHS) in $I\kappa B\alpha$ mutant mice

T cell proliferation upon stimulation with immobilized anti-CD3 with and without soluble anti-CD28 and IL-2 secretion

in response to immobilized anti-CD3 were comparable in mutant mice and WT littermates (Fig. 5, A and B). CD28 ligation increased IL-2 secretion by the mutant T cells, albeit to a significantly lower extent than in WT T cells (Fig. 5 B).

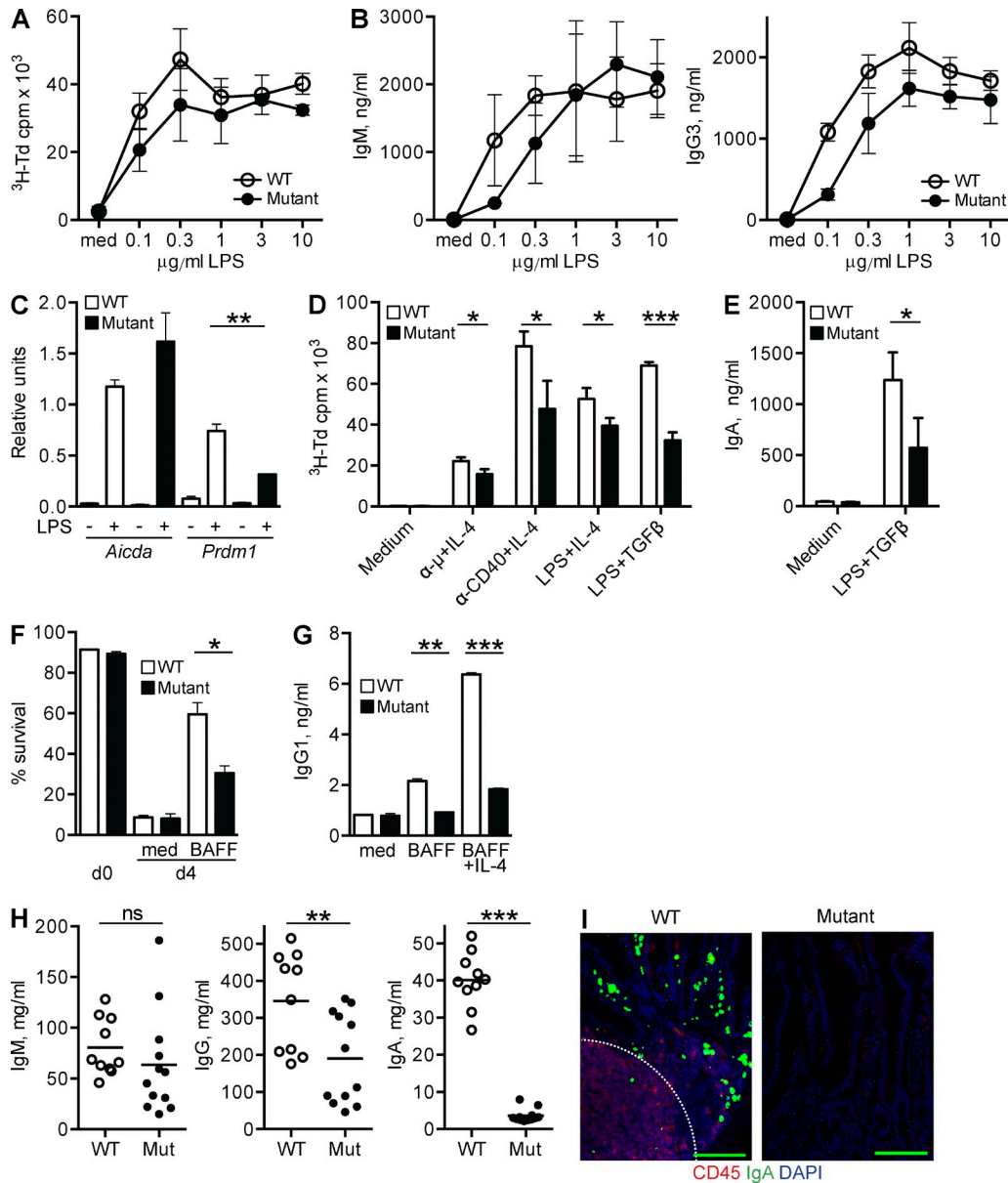


**Figure 6. B cell function in  $\kappa B\alpha$  mutant mice.** (A and B) Proliferation determined by [<sup>3</sup>H]thymidine incorporation into DNA (A) and IgM and IgG production determined by ELISA in the supernatants (B) of purified splenic B cells stimulated for 3 d with LPS. Data are representative of a minimum of four mice per group in three experiments. (C) *Aicda* and *Prdm1* mRNA expression in B cells stimulated with 10 μg/ml LPS measured by qPCR. Data are representative of three mice per group in three experiments. (D) Proliferation by purified splenic B cells stimulated with anti-μ, anti-CD40 mAb, LPS, or TGFβ in the presence of IL-4 determined by [<sup>3</sup>H]thymidine incorporation into DNA. Data are representative of a minimum of four mice per group in three experiments. (E) IgA production by purified splenic B cells stimulated with LPS + TGFβ, as determined by ELISA of supernatants. Data are representative of a minimum of four mice per group in four experiments. (F and G) B cell survival mediated by BAFF determined by analysis of trypan blue–negative cells (F) and IgG1 production determined by ELISA in the supernatants (G) by purified naive splenic B cells stimulated with BAFF in the absence or presence of IL-4 for 4 (F) or 7 (G) d. Data are representative of three mice per group in three experiments. (H) Serum Ig levels from unimmunized 6–8-wk-old mice. Data represent the mean of duplicate determinations on sera from the number of mice indicated. (I) Small intestine sections were stained by immunofluorescence for IgA, CD45, and DAPI. The dashed line delineates the edge of the PP. Bars, 100 μm. Data are representative of two independent experiments with one mouse per group. Lines and columns represent mean, and bars represent SD. \*, P < 0.05; \*\*, P < 0.01; \*\*\*, P < 0.001.

The differentiation of naive CD4<sup>+</sup> T cells in vitro under polarizing conditions into Th2 cells was comparable in the mutant and WT littermates, but differentiation into Th1 and Th17 cells was impaired in the mutant (Fig. 5 C). These findings

indicate that TCR–driven T cell proliferation, IL-2 secretion, and in vitro Th2 cell differentiation were normal in the mutant, but in vitro Th1 and Th17 cell differentiation were significantly impaired.

After i.p. immunization with OVA, T cells in splenocyte cultures from  $\text{I}\kappa\text{B}\alpha$  mutant mice proliferated normally and secreted IL-2 robustly in response to OVA stimulation (Fig. 5 D). In contrast to the response to i.p. immunization, which involves interaction in the spleen between antigen-presenting DCs and T cells, the T cell response to cutaneously introduced antigen involves interaction in the skin-draining LN between DCs that have captured antigen in the skin and recirculating antigen-specific T cells.  $\text{I}\kappa\text{B}\alpha$  mutant mice sensitized with the hapten oxazolone (OXA) developed significantly less ear swelling with markedly less cellular infiltration and expressed significantly less *Irfng* and *Il4* mRNA than WT controls (Fig. 5, E and F). Because  $\text{I}\kappa\text{B}\alpha$  mutant mice have partial intrinsic T cell defects, the absence of LNs likely plays a major role in the failure of these mice to mount a CHS response.

### B cell function is modestly decreased in vitro but severely impaired in vivo in $\text{I}\kappa\text{B}\alpha$ mutant mice

Proliferation and IgG secretion by purified total splenic B cells in response to stimulation with LPS were modestly, but significantly, reduced in the mutant, whereas IgM secretion was not significantly reduced (Fig. 6, A and B). *Aicda* (*activation-induced cytidine deaminase*) expression in LPS-stimulated B cells from the mutant was comparable with WT controls, but *Prdm1* (*PR domain zinc finger protein 1*) expression was significantly decreased (Fig. 6 C). The proliferation of splenic B cells from  $\text{I}\kappa\text{B}\alpha$  mutant mice in response to stimulation with anti-IgM + IL-4, anti-CD40 + IL-4, LPS + IL-4, and LPS + TGF $\beta$  was modestly, but significantly, decreased compared with B cells from WT littermates, as measured by [ $^3\text{H}$ ]thymidine incorporation (Fig. 6 D) and CFSE dye dilution (not depicted). IgM, but not IgG, production was significantly decreased in response to LPS + IL-4 and anti-CD40 + IL-4 (not depicted), suggesting that IL-4 may overcome some of the hyporesponsiveness of the B cells to LPS alone. LPS + TGF $\beta$  stimulation caused significantly less IgA production by mutant B cells than by WT B cells (Fig. 6 E). BAFF, which activates primarily the noncanonical NF- $\kappa\text{B}$  pathway (Claudio et al., 2002), promotes B cell survival and drives modest IgG1 isotype switching in naive B cells (Batten et al., 2000; Castigli et al., 2005). The survival of naive B cells in the presence of BAFF and their IgG1 production in response to BAFF alone or with added IL-4 were significantly reduced in  $\text{I}\kappa\text{B}\alpha$  mutant mice compared with WT littermates (Fig. 6, F and G). This is consistent with the impaired noncanonical NF- $\kappa\text{B}$  signaling in the mutant.

Serum IgM levels were comparable in mutant mice and WT littermates, whereas serum IgG levels were significantly decreased, and serum IgA was nearly absent in the mutants (Fig. 6 H). IgA $^+$  plasma cells were absent from the lamina propria of mutant mice (Fig. 6 I).

The antibody responses to the type I T-independent (TI) antigen TNP-LPS, the type II TI antigen TNP-Ficoll, and the T-dependent (TD) antigens OVA and TNP-KLH were all severely diminished in  $\text{I}\kappa\text{B}\alpha$  mutant mice compared with WT controls (Fig. 7, A–C; and not depicted). The IgG antibody

response to TD antigens requires GC formation (Rajewsky, 1996). OVA immunization resulted in the robust development of GCs in the spleens of WT mice as indicated by staining for peanut agglutinin (PNA; Fig. 7 D). In contrast, GC development was severely deficient in  $\text{I}\kappa\text{B}\alpha$  mutant mice. OVA immunization caused a significant increase in the percentage of B220 $^+$ PNA $^+$  and B220 $^+$ Fas $^+$ GL7 $^+$  GC B cells in the spleens of WT mice but not  $\text{I}\kappa\text{B}\alpha$  mutant mice (Fig. 7, E and F).

### Reconstitution of $\text{I}\kappa\text{B}\alpha$ mutant mice with WT BM fails to correct their secondary lymphoid organs and immune defects

To determine whether the immune phenotype of  $\text{I}\kappa\text{B}\alpha$  mutant mice was intrinsic to lymphocytes, we examined immune function in WT $\rightarrow$  $\text{I}\kappa\text{B}\alpha$  mutant chimeras. The same pool of BM cells from CD45.1 $^+$  WT mice was used to reconstitute irradiated CD45.2 $^+$   $\text{I}\kappa\text{B}\alpha$  mutant mice and WT littermates. 8 wk after BM transplantation, the two chimeras had comparable numbers of lymphocytes in the blood, with virtually all B cells and >80% of T cells of donor origin (not depicted). Gross examination revealed that LNs and PPs were present in WT $\rightarrow$ WT control chimeras (Fig. 8, A and B). In contrast, they were not detectable in WT $\rightarrow$  $\text{I}\kappa\text{B}\alpha$  mutant chimeras. Splenic cellularity and the percentages of CD3 $^+$ , CD4 $^+$ , CD8 $^+$ , and B220 $^+$  cells were comparable in the two chimeras (not depicted). However, follicles and FDCs, which were present in the spleens of control chimeras, were absent from WT $\rightarrow$  $\text{I}\kappa\text{B}\alpha$  mutant chimeras (Fig. 8 C), and the percentage of MZ B cells was distinctly decreased in the WT $\rightarrow$  $\text{I}\kappa\text{B}\alpha$  mutant chimeras (Fig. 8 D). These findings strongly suggest that nontransferable stromal cells are responsible for the lack of LNs, PPs, splenic follicles, and FDCs and for the decrease in MZ B cells in  $\text{I}\kappa\text{B}\alpha$  mutant mice.

Evaluation of CHS revealed significantly decreased ear swelling, inflammation, and cytokine expression in WT $\rightarrow$  $\text{I}\kappa\text{B}\alpha$  mutant chimeras compared with control chimeras (Fig. 8, E–G). WT $\rightarrow$  $\text{I}\kappa\text{B}\alpha$  mutant chimeras had impaired antibody responses to TNP-Ficoll and OVA compared with control chimeras (Fig. 8, H and I). OVA immunization resulted in the development of GCs and in a significant increase in the percentage of B220 $^+$ PNA $^+$  GC B cells in the spleens of control chimeras, but not WT $\rightarrow$  $\text{I}\kappa\text{B}\alpha$  mutant chimeras (Fig. 8, J and K). The failure of reconstitution with WT BM cells to correct the immune defects in  $\text{I}\kappa\text{B}\alpha$  mutant mice indicates that nonhematopoietic cells are major contributors to the immune deficiency in  $\text{I}\kappa\text{B}\alpha$  mutant mice.

### Secondary lymphoid organs, CHS, and GC formation, but not B cell function, are restored in $\text{I}\kappa\text{B}\alpha$ mutant $\rightarrow$ *Rag2* $^{-/-}$ chimeras

*Rag2* $^{-/-}$  mice possess LTi cells, and the cross talk between LTi cells and stromal cells is intact in these mice (Fu and Chaplin, 1999). To determine whether some of the immune defects in  $\text{I}\kappa\text{B}\alpha$  mutant mice are intrinsic to hematopoietic cells, we generated *Rag2* $^{-/-}$  chimeras. LNs were present and comparable in size, cellularity, and distribution of T and B cells in  $\text{I}\kappa\text{B}\alpha$  mutant $\rightarrow$ *Rag2* $^{-/-}$  chimeras and WT $\rightarrow$ *Rag2* $^{-/-}$  control chimeras (Fig. 9, A and B). PPs and splenic follicles

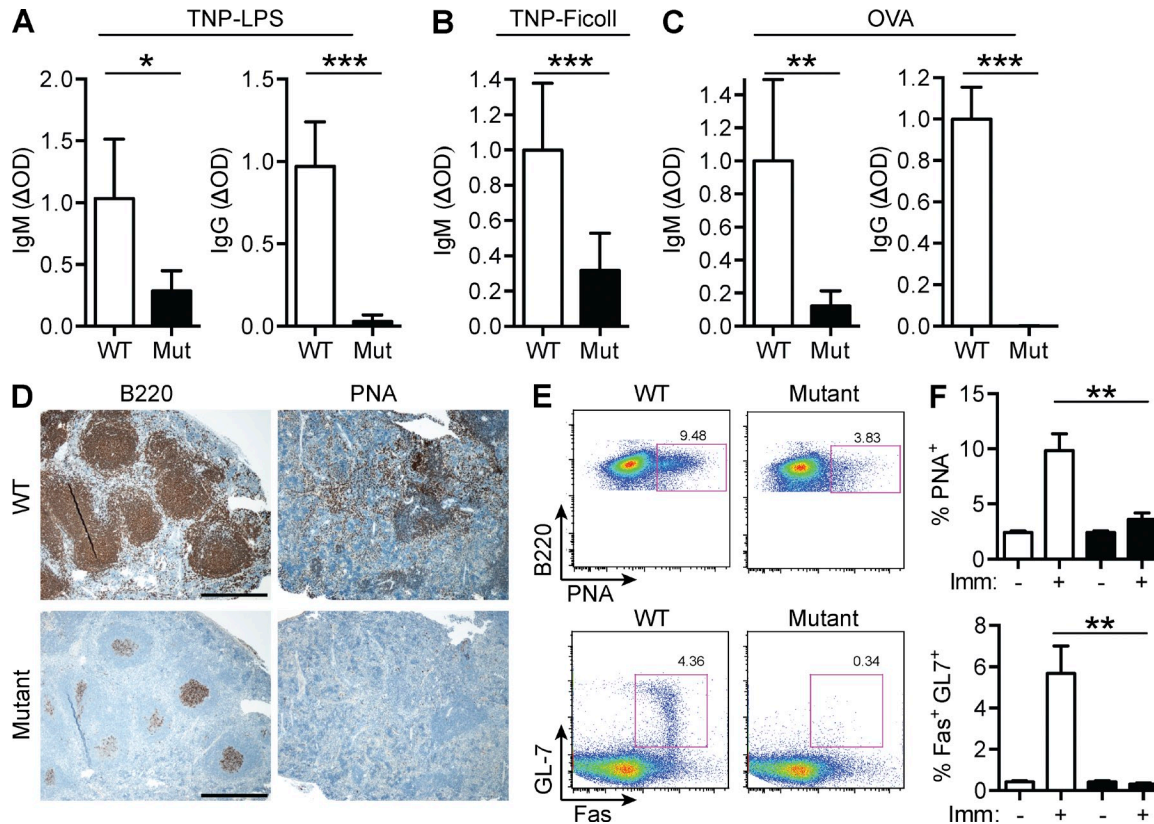


**Figure 7. Impaired antibody responses in  $\text{I}\kappa\text{B}\alpha$  mutant mice.** (A–C) TNP-specific serum Ig measured by ELISA in mice immunized with TNP-LPS (A) and TNP-Ficoll (B) and OVA-specific serum Ig measured by ELISA in mice immunized with OVA (C). Data represent the mean of duplicate determinations on sera from four to seven mice per group. (D) Spleen sections from immunized mice were stained by histochemistry with anti-B220 or PNA. Bars, 500  $\mu\text{m}$ . Data are representative of six mice per group in three independent experiments. (E and F) Analysis of PNA<sup>+</sup> and Fas<sup>+</sup>GL7<sup>+</sup> B cells among the B220<sup>+</sup> population of splenic B cells of OVA-immunized mutant mice and WT controls (E) and percentages of these subpopulations in unimmunized and OVA-immunized mice of both groups (F), as analyzed by flow cytometry. Data are representative of three to six mice per group in three independent experiments. Imm, immunization. Lines and columns represent mean, and bars represent SD in A–C and F. \*,  $P < 0.05$ ; \*\*,  $P < 0.01$ ; \*\*\*,  $P < 0.001$ .

and FDCs were also present and comparable in size in the two chimeras (Fig. 9, C and D). Furthermore, MZ B cells were present in  $\text{I}\kappa\text{B}\alpha$  mutant  $\rightarrow$   $\text{Rag}2^{-/-}$  chimeras, although their number was less than in control chimeras (Fig. 9 E). These findings indicate that the defective lymphoid organogenesis in  $\text{I}\kappa\text{B}\alpha$  mutant mice was not caused by an intrinsic defect in hematopoietic cells.

$\text{I}\kappa\text{B}\alpha$  mutant  $\rightarrow$   $\text{Rag}2^{-/-}$  chimeras mounted a CHS response to OXA comparable with that of control chimeras, as measured by ear swelling, cellular infiltration, and *Ifng* and *Il4* mRNA expression (Fig. 10, A–C). These findings strongly suggest that the lack of CHS in the  $\text{I}\kappa\text{B}\alpha$  mutants is caused by their lack of LNs.

Despite the presence of splenic follicles, FDCs, and MZ B cells, the antibody responses to TNP-LPS, TNP-Ficoll, and OVA were all significantly lower in  $\text{I}\kappa\text{B}\alpha$  mutant  $\rightarrow$   $\text{Rag}2^{-/-}$  chimeras than in control chimeras (Fig. 10, D–F). After OVA immunization, the chimeras formed splenic GCs that were comparable in size and number (Fig. 10 G) and had a comparable increase in the percentage of B220<sup>+</sup>PNA<sup>+</sup> cells (Fig. 10 H). Quantitative PCR (qPCR) analysis performed

on B220<sup>+</sup>PNA<sup>+</sup> cells revealed that mRNA levels of *Aicda* and *Bcl6*, which are expressed by GC B cells, were comparable in the two chimeras. In contrast, mRNA levels of *Prdm1* and *Xbp1* (*X-box-binding protein 1*), which drive plasma cell differentiation, were significantly lower in the  $\text{I}\kappa\text{B}\alpha$  mutant  $\rightarrow$   $\text{Rag}2^{-/-}$  chimeras than in control chimeras (Fig. 10 I). These results suggest that defective GC formation in  $\text{I}\kappa\text{B}\alpha$  mutant mice is caused by a defect in nonhematopoietic architectural cells rather than in hematopoietic cells. Nevertheless, the B cells from the mutant have an intrinsic defect in terminal differentiation into plasma cells.

## DISCUSSION

We have generated mice heterozygous for the S32I mutation in  $\text{I}\kappa\text{B}\alpha$  that recapitulate the known features of ED-ID patients who carry the same mutation. Strikingly, these mice had severely defective lymphoid organogenesis caused by a defect in nontransferable architectural cells, a finding not previously appreciated in patients, which may explain their susceptibility to infection despite normal lymphocyte number and in vitro function and their poor response to HSCT.

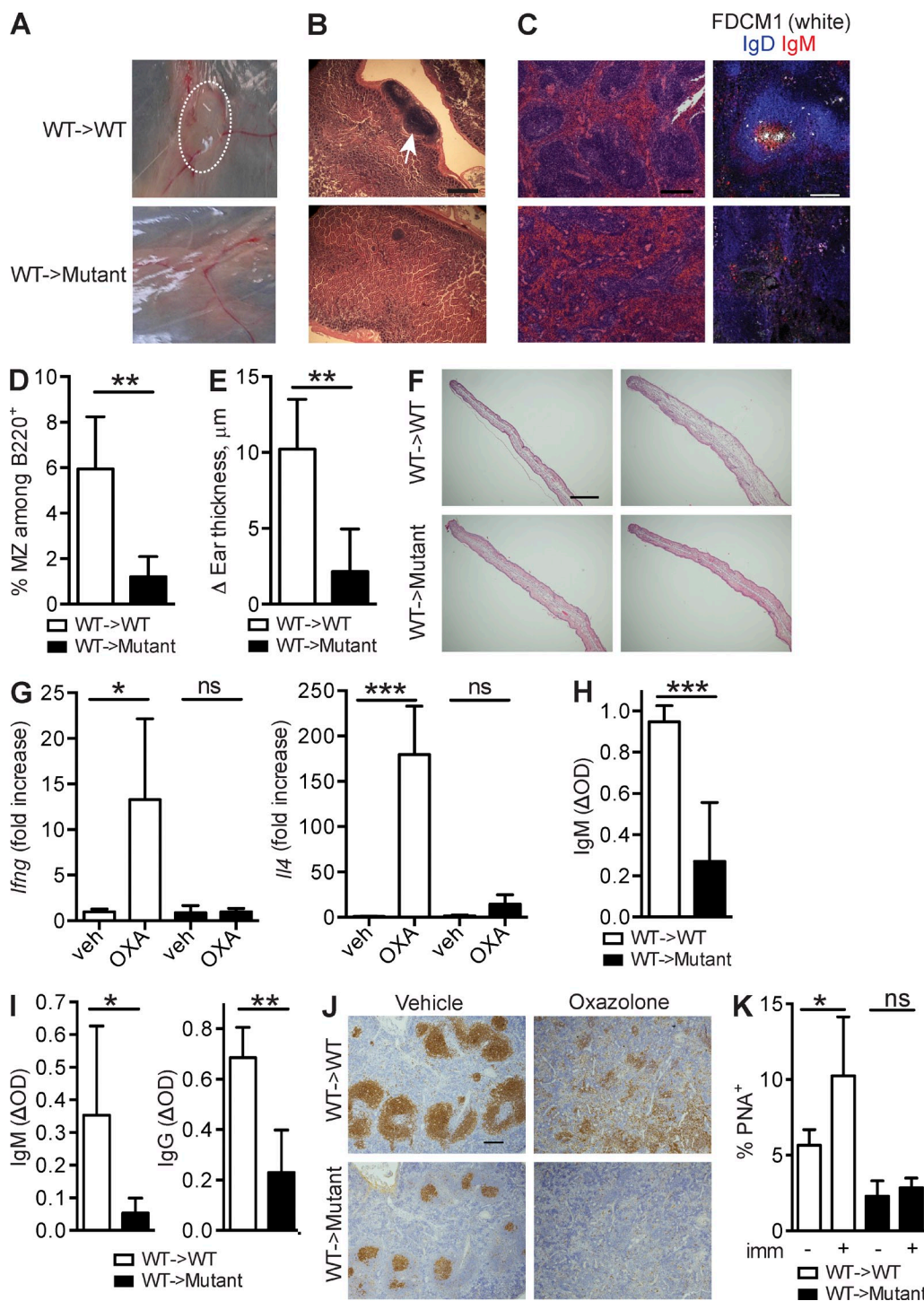


**Figure 8. Secondary lymphoid organs and immune function in WT→ $\kappa$ B $\alpha$  mutant chimeras.** (A) Photograph of inguinal fat pad with the vessel junction. The dotted circle indicates the LN at the vessel junction in the fat pad. (B) H&E staining of small intestine sections. The arrow points to a PP in the WT mouse. (C) Spleen sections were stained with H&E (left) and by immunofluorescence for FDCM1, IgD, and IgM (right). (D) Percentage of CD21<sup>+</sup>CD23<sup>-</sup> MZ B cells among B220<sup>+</sup> cells in the spleen, as determined by flow cytometry ( $n = 4-6$  mice per group). (E-G) Increase in ear thickness measured by a micrometer (E), representative H&E-stained sections (F), and *Irfng* and *Il-4* mRNA expression determined by qPCR (G) 24 h after ear challenge with OXA or vehicle ( $n = 3-5$  mice per group). (H and I) Serum TNP-specific (H) and OVA-specific (I) antibody measured by ELISA in mice immunized with TNP-Ficoll (H) and OVA (I), respectively ( $n = 5$  mice per group). (J) Spleen sections from immunized mice stained by histochemistry with anti-B220 mAb or PNA. Bars: (B) 500  $\mu$ m; (C [left], F, and J) 200  $\mu$ m; (C, right) 100  $\mu$ m. (K) Percentage of PNA<sup>+</sup> B cells among the B220<sup>+</sup> population of splenic B cells determined by flow cytometry ( $n = 3-5$  mice per group). Data in A-C and J are representative of three to six mice. Columns and bars in D, E, G-I, and K represent mean and SD. \*,  $P < 0.05$ ; \*\*,  $P < 0.01$ ; \*\*\*,  $P < 0.001$ .

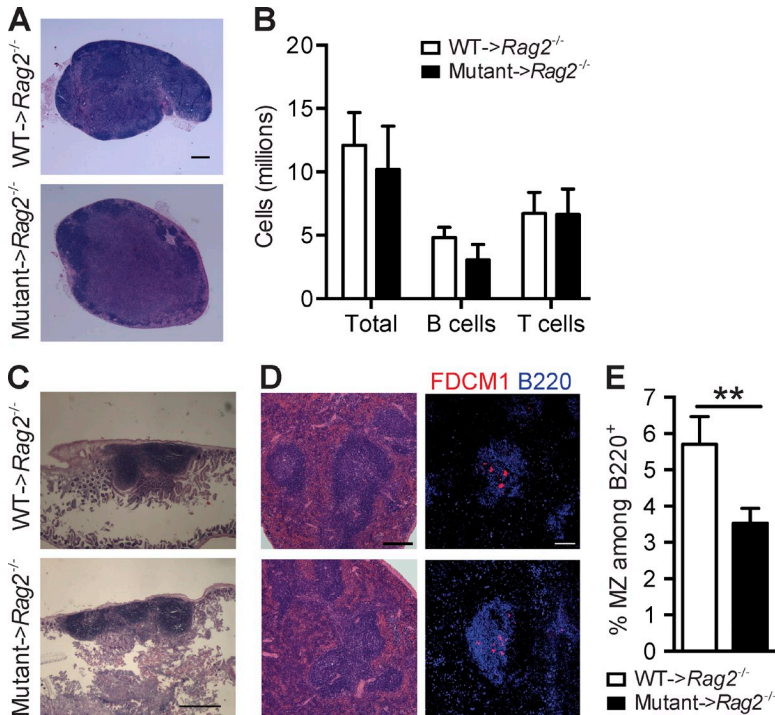


**Figure 9. Defective lymphoid organogenesis in  $I\kappa B\alpha$  mutant→ $Rag2^{-/-}$  chimeras.** (A) Inguinal LN sections stained with H&E. (B) Numbers of total cells and B and T cells from inguinal and axillary LNs (one from each mouse) evaluated by counting in a hemocytometer. (C) H&E staining of longitudinal sections of the small intestine. (D) Spleen sections were stained with H&E (left) and by immunofluorescence for B220 and FDCM1 (right). Bars: (A and D [right]) 100  $\mu$ m; (C) 1,000  $\mu$ m; (D, left) 200  $\mu$ m. (E) Percentage of CD21<sup>+</sup>CD23<sup>-</sup> MZ B cells among the B220<sup>+</sup> cells in the spleen determined by flow cytometry. Data in A–E are representative of four to six mice per group in three to four independent experiments. Columns and bars in B and E represent mean and SD. \*\*,  $P < 0.01$ .

The  $I\kappa B\alpha$  mutant mouse we generated had ectodermal defects similar to those present in EDA- and EDA-R-deficient patients and mice and in patients with ED-ID (Srivastava et al., 2001; Laurikkala et al., 2002; Clauss et al., 2008; Hanson et al., 2008; Kawai et al., 2012). Growth, weight gain, and survival were diminished in the mutant, like in patients with hypermorphic  $I\kappa B\alpha$  mutations (Courtois et al., 2003; Janssen et al., 2004; McDonald et al., 2007; Lopez-Granados et al., 2008; Ohnishi et al., 2012; Yoshioka et al., 2013). Activation of the canonical NF- $\kappa$ B pathway was deficient in these mice, as in the patients (Courtois et al., 2003; McDonald et al., 2007). This was indicated by impaired  $I\kappa B\alpha$  phosphorylation and degradation in fibroblasts after stimulation with IL-1, TNF, and LPS. The mutant also showed reduced cytokine production by BMDCs in response to TLR stimulation and decreased up-regulation of ICAM1 and VCAM1 expression by MEFs in response to TNF. Thus, the heterozygous  $I\kappa B\alpha$  mutant mice we generated represent a faithful model of humans with hypermorphic  $I\kappa B\alpha$  mutations.

Secondary lymphoid organogenesis was severely defective in the  $I\kappa B\alpha$  mutant mouse. The mutant completely lacked LNs and PPs, and its spleen lacked follicles, MZs, MZ B cells, and FDCs. This was surprising because secondary lymphoid organogenesis is relatively well preserved in p50-deficient mice, which only lack inguinal LNs (Lo et al., 2006), and partially preserved in mice deficient in TNF, TNFR1 (TNF receptor 1), RANK (receptor activator of NF- $\kappa$ B), or RANKL (RANK ligand), which signal through the canonical NF- $\kappa$ B pathway (Pasparakis et al., 1996, 1997; Körner et al., 1997; Matsumoto et al., 1997; Dougall et al., 1999; Kong et al., 1999;

Kim et al., 2000). Instead, the phenotype of  $I\kappa B\alpha$  mutant mice closely resembles that of mice deficient in RelB or NIK and mice deficient in LT $\alpha$ , LT $\beta$ , or LT $\beta$ R, which signal through both the canonical and noncanonical NF- $\kappa$ B pathways (Miyawaki et al., 1994; Banks et al., 1995; Weih et al., 1995; Koike et al., 1996; Koni et al., 1997; Fütterer et al., 1998; Weih et al., 2001; Tumanov et al., 2003; Seymour et al., 2006).

Defective lymphoid organogenesis has not been previously appreciated in patients with ED-ID. However, tonsils and cervical LNs have been noted to be absent in at least one of the patients with the S32I  $I\kappa B\alpha$  mutation (Dupuis-Girod et al., 2006). Circulating lymphocyte counts were significantly elevated in  $I\kappa B\alpha$  mutant mice, as has been noted in patients with  $I\kappa B\alpha$  deficiency (Courtois et al., 2003; Janssen et al., 2004; McDonald et al., 2007; Ohnishi et al., 2012) and in mice that lack LNs and PPs (De Togni et al., 1994; Alimzhanov et al., 1997; Fütterer et al., 1998).

Lymphoid organogenesis involves activation of both the canonical and noncanonical NF- $\kappa$ B pathways through LT $\alpha$ 1 $\beta$ 2-LT $\beta$ R interactions between LT $i$  cells and stromal organizer cells (Mebius, 2003; Vondenhoff et al., 2009; van de Pavert and Mebius, 2010; Roozendaal and Mebius, 2011). LT $i$  cells were present in the  $I\kappa B\alpha$  mutant, consistent with previous observations in mice with defects in the canonical NF- $\kappa$ B pathway (Alcamo et al., 2002). As expected, MEFs from the mutant failed to up-regulate *Vcam1*, *Icam1*, and *Cxcl10* mRNA expression in response to LT $\beta$ R ligation, which depends on the canonical NF- $\kappa$ B pathway (Dejardin et al., 2002; Caposio et al., 2007). In addition, they failed to up-regulate the expression of *Madcam1*, which depends on the noncanonical pathway downstream of

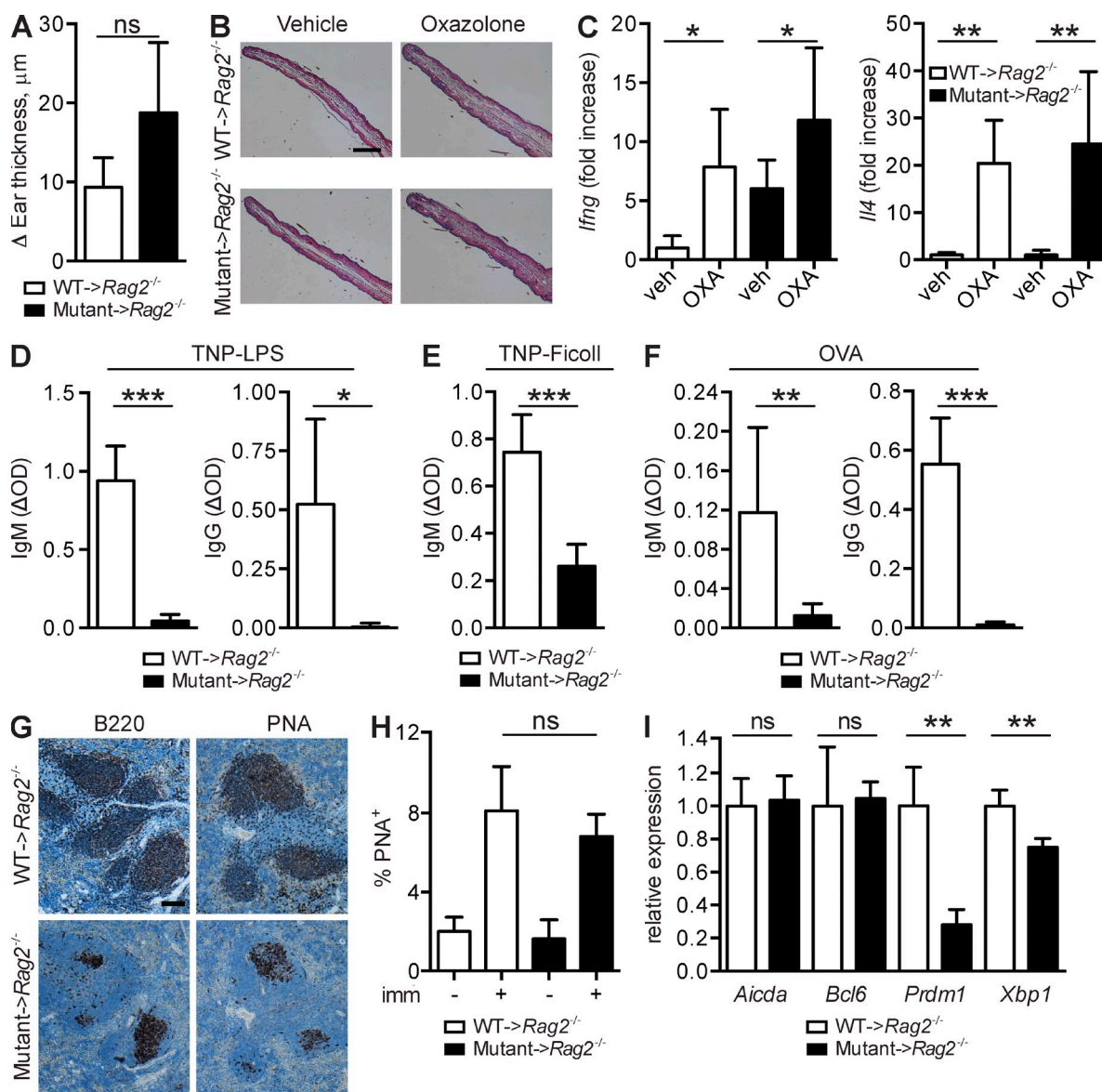


**Figure 10. Defective immune function in  $I\kappa B\alpha$  mutant  $\rightarrow Rag2^{-/-}$  chimeras.** (A–C) Increase in ear thickness measured by a micrometer (A), representative H&E-stained sections (B), and *Irfng* and *Il-4* mRNA expression determined by qPCR (C) 24 h after ear challenge with OXA or vehicle. Data in A–C are representative of five to seven mice per group in three experiments. (D–F) Serum TNP-specific (D and E) and OVA-specific (F) antibody measured by ELISA in mice immunized with TNP-LPS (D), TNP-Ficoll (E), and OVA (F), respectively. Data in D–F are representative of a mean of two determinations on sera from 5–10 mice per group. (G) Spleen sections from immunized mice stained by histochemistry with anti-B220 or PNA. Bars: (B) 200  $\mu\text{m}$ ; (G) 25  $\mu\text{m}$ . (H) Percentage of PNA<sup>+</sup> B cells among the B220<sup>+</sup> population of splenic B cells ( $n = 3$  mice per group) determined by flow cytometry. (I) *Aicda*, *Bcl6*, *Prdm1*, and *Xbp1* mRNA expression in B220<sup>+</sup>PNA<sup>+</sup> cells from immunized mice measured by qPCR. Data in G–I are representative of three mice per group in three experiments. Columns and bars in A, C–F, H, and I represent mean and SD. \*,  $P < 0.05$ ; \*\*,  $P < 0.01$ ; \*\*\*,  $P < 0.001$ .

LT $\beta$ R (Ganeff et al., 2011). Furthermore, splenocytes from the  $I\kappa B\alpha$  mutant expressed significantly less mRNA for the chemokine genes *Cd19*, *Cxd12*, and *Cxd13*, the expression of which depends on the noncanonical NF- $\kappa$ B pathway (Dejardin et al., 2002). We demonstrated that the levels of p100 were markedly reduced in cells from the mutant. This is consistent with previous observations that canonical NF- $\kappa$ B signaling controls p100 levels in cell lines (Liptay et al., 1994; Dejardin et al., 2002; Shih et al., 2011). Because canonical NF- $\kappa$ B activation is not required

for p100 processing into its active product p52 (Dejardin et al., 2002), the impaired noncanonical NF- $\kappa$ B pathway activity in the mutant is likely caused by the decreased p100 levels.

In addition to the control of p100 level by the canonical pathway, there is cross talk at other levels between the canonical and noncanonical NF- $\kappa$ B pathways (Matsushima et al., 2001; Shih et al., 2011). The complexity of this talk may account for the variable effects of deficiency in individual components of the canonical NF- $\kappa$ B pathway on lymphoid

organogenesis. Thus, although lymphoid organogenesis is absent in *Rela*<sup>-/-</sup> mice rescued from lethality by breeding on the *Tnfr1*<sup>-/-</sup> background (Alcamo et al., 2002), it is relatively unaffected in p50-deficient *Nfkb1*<sup>-/-</sup> mice. NEMO-deficient patients are known to possess LNs (Orange et al., 2004; Imamura et al., 2011). A recent study demonstrates increased baseline levels of NIK and increased activation of the non-canonical pathway in NEMO-deficient MEFs caused by loss of the IKK complex (Gray et al., 2014). Although not discussed in that study, p100 levels were low in these MEFs. Increased NIK levels and activity in NEMO deficiency may compensate for the low levels of p100. In contrast, NIK levels were not increased in MEFs from the  $\text{I}\kappa\text{B}\alpha$  mutant mice.

Thymocyte development and splenic T cell numbers were normal in the  $\text{I}\kappa\text{B}\alpha$  mutant. Moreover, T cell proliferation and IL-2 secretion in response to TCR ligation with anti-CD3 or antigen stimulation after i.p. immunization were normal in the mutant. However, up-regulation of IL-2 secretion by CD28 ligation and in vitro differentiation of naive T cells into Th1 and Th17, but not Th2 cells, were impaired. The CHS response, which largely depends on T cells (Wang et al., 2000; Gorbachev and Fairchild, 2004), was markedly deficient in the mutant. Failure to mount a CHS response also occurs in *Ltbr*<sup>-/-</sup> mice (Rennert et al., 2001) and is likely caused by the absence of LNs, where contact between hapten-specific T cells and hapten-bearing DCs takes place. This is supported by the observation that the CHS response was reconstituted in  $\text{I}\kappa\text{B}\alpha$  mutant→*Rag2*<sup>-/-</sup> chimeras, which developed LNs that were normal in size and cellularity.

The  $\text{I}\kappa\text{B}\alpha$  mutant had normal B cell development in the BM and normal B cell numbers in the spleen, but had a severe deficiency in splenic MZ B cells. Proliferation of mutant B cells to LPS was normal, but proliferation to response to BCR, CD40, and TLR4 ligation in the presence of IL-4 was modestly reduced, suggesting a role for  $\text{I}\kappa\text{B}\alpha$  in B cell proliferation supported by IL-4. B cells from the mutant secreted less IgG after LPS stimulation and less IgA after LPS + TGF $\beta$  stimulation than control B cells. Expression of *Aicda* was normal, but expression of *Prdm1* was reduced in LPS-stimulated B cells from the mutant, suggesting a defect in terminal B cell differentiation. B cell survival and IgG1 isotype switching in response to BAFF, which activates NF- $\kappa$ B primarily via the canonical pathway, was impaired in the mutant. Serum IgG levels were decreased in the mutant mice, and serum IgA and intestinal IgA<sup>+</sup> cells were virtually undetectable. IgA levels are low in patients with the  $\text{I}\kappa\text{B}\alpha$  S32I mutation (Courtois et al., 2003; Janssen et al., 2004). Serum IgA is virtually absent in *Ltbr*<sup>-/-</sup> and NIK-deficient mice (Shinkura et al., 1999), and its level is decreased in *Nfkb1*<sup>-/-</sup> mice (Snapper et al., 1996) and *Rela*<sup>-/-</sup>/*Tnfr1*<sup>-/-</sup> mice, which have impaired canonical signaling (Alcamo et al., 2002). Thus, defects in both canonical and noncanonical pathways may underlie the absence of IgA in the mutant.

Antibody responses to TI and TD antigens were severely deficient in the mutant. The defective response to TNP-Ficoll is consistent with the virtual absence of MZ B cells, which play a critical role in the antibody response to type II TI antigens

(Balázs et al., 2002; Pillai et al., 2005). Remarkably, despite intact proliferation of splenic T cells in response to OVA stimulation ex vivo, the antibody response of the mutant to i.p. immunization with OVA was virtually absent and was accompanied by a total failure to form GCs. None of the antibody responses were restored in  $\text{I}\kappa\text{B}\alpha$  mutant→*Rag2*<sup>-/-</sup> chimeras, despite the restoration of MZ B cells and GC formation with generation of normal numbers of PNA<sup>+</sup> B cells, suggesting that an intrinsic defect in terminal B cell differentiation exists in the mutant. This was supported by the observation that the expression by PNA<sup>+</sup> cells of *Prdm1* and *Xbp1*, which encode two transcription factors required for plasma cell differentiation, was significantly reduced in the  $\text{I}\kappa\text{B}\alpha$  mutant→*Rag2*<sup>-/-</sup> chimeras. Thus, the defective antibody response of  $\text{I}\kappa\text{B}\alpha$  mutant mice is two-tiered, involving defective lymphoid organogenesis and an intrinsic defect in terminal B cell differentiation.

Reconstitution of the  $\text{I}\kappa\text{B}\alpha$  mutant with WT BM cells failed to restore lymphoid organogenesis and to correct the immune defects in irradiated  $\text{I}\kappa\text{B}\alpha$  mutant recipients, despite excellent chimerism in the T and B cell lineages. This finding recapitulates the poor results of allogeneic HSCT in patients with  $\text{I}\kappa\text{B}\alpha$  mutations despite the engraftment of donor lymphocytes. Notably, despite 100% chimerism in lymphoid cells, the single patient with the S32I  $\text{I}\kappa\text{B}\alpha$  mutation who has survived HSCT continues to suffer from recurrent infections requiring gamma globulin replacement and has persistent lymphocytosis, no visible tonsillar tissue, and no palpable LNs even during infection (Dupuis-Girod et al., 2006; Cancrini, C., personal communication).

Our findings suggest that defects in architectural nonhematopoietic cells, likely a mesenchymally derived stromal cell, underlie the immune deficiency in patients with ED-ID caused by mutations in  $\text{I}\kappa\text{B}\alpha$  and explain the poor outcome of allogeneic HSCT in these patients. Strategies that correct defective architectural cell function, such as implantation of stromal cell-embedded biocompatible scaffolds to generate LNs (Okamoto et al., 2007), may be valuable in patients with  $\text{I}\kappa\text{B}\alpha$  deficiency.

## MATERIALS AND METHODS

**Generation of heterozygous  $\text{I}\kappa\text{B}\alpha$  S32I knock-in mice.** The arms of the  $\text{I}\kappa\text{B}\alpha$  S32I targeting vector were amplified by PCR from genomic DNA of the CJ7 embryonic stem (ES) cell line derived from the 129Sv mouse strain. The 2.8-kb 5' and 3.1-kb 3' arms were cloned into the pKS-neo-DTAIII vector (a gift from the laboratory of M. Greenberg, Harvard Medical School, Boston, MA), and the nucleic acid G94T mutation was introduced by site-directed mutagenesis (Agilent Technologies) into exon 1 in the 5' arm, resulting in the amino acid S32I mutation (Fig. S1 A). The linearized targeting construct was electroporated into CJ7 ES cells, which were then selected in 0.4 mg/ml G418 and 10 mg/ml ganciclovir. An ES cell clone containing a disrupted allele and no random integration of the neomycin-resistance gene was confirmed by PCR and Southern blotting (Fig. S1 B) and then injected into 3.5-d-old C57BL/6 blastocysts, and  $\text{I}\kappa\text{B}\alpha$  S32I heterozygous neo mice were obtained by standard methods (Tsitsikov et al., 1997). The presence of mutant RNA was confirmed by amplifying cDNA with the primers 5'-CAGGACTGGGC-CATGGAG-3' and 5'-ATCTCCCGCAGCTCCTTC-3', followed by digestion with the restriction enzyme MwoI (Fig. S1 C).

Mice were backcrossed nine generations to C57BL/6 mice from Charles River. All mice were kept in a specific pathogen-free environment in autoclaved

cages with trimethoprim/sulfamethoxazole and enrofloxacin added to the water to prevent infection. Procedures were performed in accordance with the Animal Care and Use Committee of the Children's Hospital Boston.

**Dermal fibroblast isolation and culture.** Primary dermal fibroblasts were isolated as in McDonald et al. (2007) and grown in RPMI media plus 10% FCS (Hyclone) plus L-glutamine, penicillin, and streptomycin (Invitrogen). Fibroblasts were stimulated with media, 10 ng/ml IL-1, 10 ng/ml TNF (R&D Systems), or 1 mg/ml LPS (Sigma-Aldrich) for the indicated times.

**Western blotting.** Western blotting was performed as previously described (McDonald et al., 2007) using anti-phospho I $\kappa$ B $\alpha$  (Cell Signaling Technology), anti-mouse full-length I $\kappa$ B $\alpha$  (Abcam), and anti-actin (Sigma-Aldrich) according to the manufacturers' recommendations. Immunoblotting was also performed using anti-p100/p52, RelB, and NIK (Cell Signaling Technology). Sheep anti-mouse horseradish peroxidase-conjugated and sheep anti-rabbit horseradish peroxidase-conjugated secondary antibodies were obtained from GE Healthcare. Quantification was performed using the public domain ImageJ/Fiji software from the National Institutes of Health.

**BMDC isolation and TLR ligand stimulation.** BM was flushed from the femur and tibia of 6–8-wk-old mice, plated in DMEM (Gibco) plus 10% FCS and plus L-glutamine, penicillin, and streptomycin, 10 ng/ml GM-CSF, and 10 ng/ml IL-4. Cells were washed at day 1, replated at day 7, and used for experiments between days 8 and 12. The DC phenotype was confirmed by flow cytometry for CD11c and MHCII and negative for Ly6G. The TLR ligands PAM3CSK4 (TLR1/2), ultrapure LPS from *Salmonella minnesota* (TLR4), loxoribine (TLR7), and CpG DNA (ODN1826; TLR9) were obtained from InvivoGen.

**MEF isolation and culture.** Primary MEFs were isolated as in Xu (2005) and grown in DMEM plus 10% FCS and plus L-glutamine, penicillin, and streptomycin.

**VCAM1 surface staining.** MEFs were treated for 24 h with 10 ng/ml TNF, dissociated with trypsin/EDTA, and stained with anti-VCAM1 (eBioscience).

**LN detection by Evan's blue injection.** LN detection was performed as described in Harrell et al. (2008).

**H&E staining.** Samples of inguinal fat pad, small intestine, nasal cavity, thymus, spleen, and LN were fixed in formalin for 24 h, and then H&E staining of paraffin-embedded cut sections was performed by the Rodent Histopathology and Specialized Histopathology Services cores at the Dana Farber/Harvard Cancer Center (Boston, MA) or by Histo-Scientific Research Laboratories (HSRL, Mt. Jackson, Virginia).

**Complete blood counts (CBCs).** Blood was collected from the facial vein, and CBC analysis was performed by the Animal Research at Children's Hospital (ARCH) facility.

**FACS analysis.** Single-cell suspensions from spleen, thymus, or BM of 4–6-wk-old mice were stained with FITC, PE, PE-Cy7, APC, PerCP-Cy5.5, Alexa Fluor 700, or APC-eFluor 780-labeled mAbs and analyzed on a FACSCanto (BD). Antibodies to B220, CD3, IgM, CD21, CD23, CD93, CD43, CD4, CD8, GL-7, CD11b, Ly6G, F4/80, NK1.1, CD45, IL7-R, CD45.1, and CD45.2 were from eBioscience, mAb to Fas was from BD, and FITC-conjugated PNA was from Sigma-Aldrich.

**Immunofluorescence.** Immunofluorescence was performed as described in Cariappa et al. (2009) and Kranich et al. (2008).

**LTi cell isolation from embryonic intestine.** Embryonic intestines were isolated from E17.5 fetuses, incubated in Liberase (Roche) for 1 h at 37°C, and then passed through a 70- $\mu$ m filter. A portion of the embryos was reserved for genotyping.

**qPCR.** MEFs were stimulated with 2  $\mu$ g/ml anti-LT $\beta$ R agonist antibody AFH6 (a gift from J. Browning, Biogen Idec, Cambridge, MA) or 10 ng/ml TNF (R&D Systems) for 24 h, and RNA was extracted using the TRIzol (Invitrogen) method. cDNA was synthesized using iScript (Bio-Rad Laboratories), and qPCR was performed using TaqMan probes and the 7300 Real-time PCR System (Applied Biosystems).

**Purification and stimulation of splenic T and B cells.** T cells were purified from spleen suspensions using the pan-T cell isolation kit II (Miltenyi Biotec), and 100,000 per 96 wells were plated, along with 300,000 irradiated (3,000 rad) non-T cell APCs purified by the CD90.2 kit (Miltenyi Biotec) using RPMI supplemented with penicillin/streptomycin, HEPES (Gibco), sodium pyruvate, and  $\beta$ -mercaptoethanol (Sigma-Aldrich). Plates were coated with 0.25–4  $\mu$ g/ml anti-CD3 (clone 145-2C11; eBioscience) at 37°C for 1 h and washed with PBS, and cells were then cultured with or without the addition of 1  $\mu$ g/ml anti-CD28 (clone 37.51; eBioscience). Cells were also stimulated with 200  $\mu$ g/ml OVA (Sigma-Aldrich). Tritiated thymidine was added on day 3, and incorporation was assayed after 15–18 h. IL-2 production was assayed from day 2 supernatants by ELISA (eBioscience).

Assays for B cell proliferation, Ig production, and GC formation were performed as previously described (Koduru et al., 2010). In brief, B cells were purified from spleen suspensions using anti-CD43 microbeads (Miltenyi Biotec), resuspended in RPMI supplemented with penicillin/streptomycin, HEPES, sodium pyruvate, and  $\beta$ -mercaptoethanol. 200,000 cells in 96-well plates were plated for proliferation assays, and 250,000 per 24-well plates for in vitro Ig analysis. Cells were stimulated with 0.1–10  $\mu$ g/ml LPS (Sigma-Aldrich) or 10  $\mu$ g/ml LPS, 10  $\mu$ g/ml anti- $\mu$  (Jackson Immuno-Research Laboratories, Inc.), or 500 ng/ml anti-CD40 (eBioscience), alone or in combination with 40 ng/ml IL-4 (R&D Systems). Tritiated thymidine (PerkinElmer) was added at day 3, and incorporation was assayed after 15–18 h. Supernatants from in vitro Ig experiments were analyzed by ELISA on day 6. *Aicda* and *Prdm1* mRNA expression was assessed by PCR on RNA extracted from 4-d-cultured naive B cells either in medium or plus 10  $\mu$ g/ml LPS using TaqMan probes. For BAFF-induced responses, naive B cells were prepared from splenocytes by negative selection using a cocktail of biotin-conjugated mAbs to CD43, CD11b, Thy1.2, CD138, IgG1, IgG2a, IgG2b, IgG3, IgA, and IgE (BD) and streptavidin magnetic beads (Invitrogen). Naive B cells were cultured in medium alone or in the presence of 1 mg/ml sBAFF (Alexis) or 50 ng/ml sBAFF + IL-4. To assess cell viability, cells were counted at day 4 in the presence of trypan blue (Sigma-Aldrich), and the percentage of live cells was determined. IgG1 secretion in supernatants was analyzed by ELISA on day 7.

**In vitro T helper cell differentiation.** For Th0 conditions, naive CD4<sup>+</sup> T cells were sorted by MACS and were stimulated for 5 d with plate-bound antibodies against CD3 (145-2C11; 2  $\mu$ g/ml; eBioscience) and CD28 (PV-1; 2  $\mu$ g/ml; BioLegend). For Th2 cell differentiation, 50 ng/ml IL-4 (BioLegend) and 10  $\mu$ g/ml neutralizing anti-IFN- $\gamma$  mAb (XMG 1.2; BioLegend) were added. For Th17 cell differentiation, 40 ng/ml IL-6 (BioLegend), 40 ng/ml IL-23 (R&D Systems), 1 ng/ml TGF- $\beta$  (BioLegend), 10  $\mu$ g/ml anti-IL-4 (11B11; BioLegend), and 10  $\mu$ g/ml anti-IFN- $\gamma$  (XMG 1.2; BioLegend) neutralizing antibodies were added. For Th1 cell differentiation, 5 ng/ml IL-12 (BioLegend) and 10  $\mu$ g/ml anti-IL-4 neutralizing mAbs (11B11; BioLegend) were added.

**Serum Ig levels and antibody responses.** 4–6-wk-old mice were immunized i.p. with 50  $\mu$ g OVA with Alum (Sigma-Aldrich) in PBS at day 0, boosted at day 14, and bled at days 0 and 21. Mice were immunized i.p. with 25  $\mu$ g TNP-LPS (Biosearch Technologies) in PBS or with 25  $\mu$ g TNP-Ficoll (Biosearch Technologies) at day 0 and bled at days 0 and 14. Antigen-specific antibody responses were analyzed by OVA- or TNP-specific ELISA using 96-well plates coated with either OVA- or TNP-conjugated BSA (Biosearch Technologies) at 10  $\mu$ g/ml in PBS. For serum Ig levels, plates were coated with isotype-specific antibodies (SouthernBiotech). AP-conjugated secondary antibodies (SouthernBiotech) and PNPP (Sigma-Aldrich) were used for ELISA.

**CHS to OXA.** Mice were sensitized by the application of 100  $\mu$ l of 2% OXA (Sigma-Aldrich) in ethanol on day 1 to shaved abdominal skin. On day 5, the left ear was challenged with 10  $\mu$ l of 1% OXA, and the right ear was challenged with vehicle (ethanol) on dorsal and ventral surfaces. Ear thickness was measured after 24 h with a micrometer (Mitutoyo).

**BM reconstitution of mutant mice.** Adult healthy mutant mice and their WT littermates received two 550-cGy ( $^{137}$ Cesium source) doses of total body irradiation 3 h apart. BM was collected from CD45.1 mice (Charles River), and  $10^5$  viable BM cells were injected i.v. into the mice. Reconstitution was assessed by flow cytometry using antibodies to CD45.1 (donor) and CD45.2 (recipient).

**BM reconstitution of *Rag2*<sup>-/-</sup> mice.** BM was collected from 6-wk-old mutant mice or their WT littermates. Flow cytometry was performed to assure the CD34<sup>+</sup> population was comparable between WT and mutant BM. Adult *Rag2*<sup>-/-</sup> recipient mice received a single 250-cGy dose of total body irradiation. Viability of the BM cells was examined by trypan blue dye exclusion, and  $10^5$  viable BM cells were injected i.v. into the *Rag2*<sup>-/-</sup> mice.

**PNA<sup>+</sup> B cell sorting.** 10 d after immunization with OVA plus alum, spleens from *Rag2*<sup>-/-</sup> BM chimeras were harvested and stained for B220 and PNA. Double-positive cells were collected at the Children's Hospital cell sorting core.

**Statistical analysis.** Statistical analysis of data was performed with Prism software (GraphPad Software) using the Student's *t* test or ANOVA.

**Online supplemental material.** Fig. S1 shows the *Nfkb1a* targeting construct and screening strategy. Online supplemental material is available at <http://www.jem.org/cgi/content/full/jem.20140979/DC1>.

We thank Dr. Talal Chatila for critical reading of the manuscript, the members of the Geha laboratory for support, and Drs. Shiv Pillai, Luigi Notarangelo, and Koichi Kobayashi for their advice.

This work was supported by National Institutes of Health (NIH) grants 5P01AI076210 and 5T32-AI007512 to R.S. Geha and by a Talecris fellowship to J.L. Mooster.

The authors declare no competing financial interests.

Submitted: 22 May 2014

Accepted: 23 December 2014

## REFERENCES

- Alcamo, E., N. Hacohen, L.C. Schulte, P.D. Rennert, R.O. Hynes, and D. Baltimore. 2002. Requirement for the NF- $\kappa$ B family member RelA in the development of secondary lymphoid organs. *J. Exp. Med.* 195:233–244. <http://dx.doi.org/10.1084/jem.20011885>
- Alimzhanov, M.B., D.V. Kuprash, M.H. Kosco-Vilbois, A. Luz, R.L. Turetskaya, A. Tarakhovskiy, K. Rajewsky, S.A. Nedospasov, and K. Pfeffer. 1997. Abnormal development of secondary lymphoid tissues in lymphotoxin  $\beta$ -deficient mice. *Proc. Natl. Acad. Sci. USA.* 94:9302–9307. <http://dx.doi.org/10.1073/pnas.94.17.9302>
- Balázs, M., F. Martin, T. Zhou, and J. Kearney. 2002. Blood dendritic cells interact with splenic marginal zone B cells to initiate T-independent immune responses. *Immunity.* 17:341–352. [http://dx.doi.org/10.1016/S1074-7613\(02\)00389-8](http://dx.doi.org/10.1016/S1074-7613(02)00389-8)
- Banks, T.A., B.T. Rouse, M.K. Kerley, P.J. Blair, V.L. Godfrey, N.A. Kuklin, D.M. Bouley, J. Thomas, S. Kanangat, and M.L. Mucenski. 1995. Lymphotoxin- $\alpha$ -deficient mice. Effects on secondary lymphoid organ development and humoral immune responsiveness. *J. Immunol.* 155:1685–1693.
- Batten, M., J. Groom, T.G. Cachero, F. Qian, P. Schneider, J. Tschopp, J.L. Browning, and F. Mackay. 2000. BAFF mediates survival of peripheral immature B lymphocytes. *J. Exp. Med.* 192:1453–1466. <http://dx.doi.org/10.1084/jem.192.10.1453>
- Bénézech, C., A. White, E. Mader, K. Serre, S. Parnell, K. Pfeffer, C.F. Ware, G. Anderson, and J.H. Caamaño. 2010. Ontogeny of stromal organizer cells during lymph node development. *J. Immunol.* 184:4521–4530. <http://dx.doi.org/10.4049/jimmunol.0903113>
- Bonizzi, G., and M. Karin. 2004. The two NF- $\kappa$ B activation pathways and their role in innate and adaptive immunity. *Trends Immunol.* 25:280–288. <http://dx.doi.org/10.1016/j.it.2004.03.008>
- Bren, G.D., N.J. Solan, H. Miyoshi, K.N. Pennington, L.J. Pobst, and C.V. Paya. 2001. Transcription of the RelB gene is regulated by NF- $\kappa$ B. *Oncogene.* 20:7722–7733. <http://dx.doi.org/10.1038/sj.onc.1204868>
- Caposio, P., T. Musso, A. Luganini, H. Inoue, M. Gariglio, S. Landolfo, and G. Gribaudo. 2007. Targeting the NF- $\kappa$ B pathway through pharmacological inhibition of IKK2 prevents human cytomegalovirus replication and virus-induced inflammatory response in infected endothelial cells. *Antiviral Res.* 73:175–184. <http://dx.doi.org/10.1016/j.antiviral.2006.10.001>
- Cariappa, A., H. Takematsu, H. Liu, S. Diaz, K. Haider, C. Boboila, G. Kalloo, M. Connole, H.N. Shi, N. Varki, et al. 2009. B cell antigen receptor signal strength and peripheral B cell development are regulated by a 9-O-acetyl sialic acid esterase. *J. Exp. Med.* 206:125–138. <http://dx.doi.org/10.1084/jem.20081399>
- Castigli, E., S.A. Wilson, S. Scott, F. Dedeoglu, S. Xu, K.P. Lam, R.J. Bram, H. Jabara, and R.S. Geha. 2005. TACI and BAFF-R mediate isotype switching in B cells. *J. Exp. Med.* 201:35–39. <http://dx.doi.org/10.1084/jem.20032000>
- Chen, K., E.M. Coonrod, A. Kumánovics, Z.F. Franks, J.D. Durtschi, R.L. Margraf, W. Wu, N.M. Heikal, N.H. Augustine, P.G. Ridge, et al. 2013. Germline mutations in NFKB2 implicate the noncanonical NF- $\kappa$ B pathway in the pathogenesis of common variable immunodeficiency. *Am. J. Hum. Genet.* 93:812–824. <http://dx.doi.org/10.1016/j.ajhg.2013.09.009>
- Claudio, E., K. Brown, S. Park, H. Wang, and U. Siebenlist. 2002. BAFF-induced NEMO-independent processing of NF- $\kappa$ B2 in maturing B cells. *Nat. Immunol.* 3:958–965. <http://dx.doi.org/10.1038/ni842>
- Clauss, F., M.C. Manière, F. Obry, E. Waltmann, S. Hadj-Rabia, C. Bodemer, Y. Alembik, H. Lesot, and M. Schmittbuhl. 2008. Dento-craniofacial phenotypes and underlying molecular mechanisms in hypohidrotic ectodermal dysplasia (HED): a review. *J. Dent. Res.* 87:1089–1099. <http://dx.doi.org/10.1177/154405910808701205>
- Courtois, G., A. Smahi, J. Reichenbach, R. Döffinger, C. Cancrini, M. Bonnet, A. Puel, C. Chable-Bessia, S. Yamaoka, J. Feinberg, et al. 2003. A hypermorphic I $\kappa$ B $\alpha$  mutation is associated with autosomal dominant anhidrotic ectodermal dysplasia and T cell immunodeficiency. *J. Clin. Invest.* 112:1108–1115. <http://dx.doi.org/10.1172/JCI18714>
- De Togni, P., J. Goellner, N.H. Ruddle, P.R. Streeter, A. Fick, S. Mariathasan, S.C. Smith, R. Carlson, L.P. Shornick, J. Strauss-Schoenberger, et al. 1994. Abnormal development of peripheral lymphoid organs in mice deficient in lymphotoxin. *Science.* 264:703–707. <http://dx.doi.org/10.1126/science.8171322>
- Dejardin, E., N.M. Droin, M. Delhase, E. Haas, Y. Cao, C. Makris, Z.W. Li, M. Karin, C.F. Ware, and D.R. Green. 2002. The lymphotoxin- $\beta$  receptor induces different patterns of gene expression via two NF- $\kappa$ B pathways. *Immunity.* 17:525–535. [http://dx.doi.org/10.1016/S1074-7613\(02\)00423-5](http://dx.doi.org/10.1016/S1074-7613(02)00423-5)
- Dougall, W.C., M. Glaccum, K. Charrier, K. Rohrbach, K. Brasel, T. De Smedt, E. Daro, J. Smith, M.E. Tometsko, C.R. Maliszewski, et al. 1999. RANK is essential for osteoclast and lymph node development. *Genes Dev.* 13:2412–2424. <http://dx.doi.org/10.1101/gad.13.18.2412>
- Dupuis-Girod, S., C. Cancrini, F. Le Deist, P. Palma, C. Bodemer, A. Puel, S. Livadiotti, C. Picard, X. Bossuyt, P. Rossi, et al. 2006. Successful allogeneic hemopoietic stem cell transplantation in a child who had anhidrotic ectodermal dysplasia with immunodeficiency. *Pediatrics.* 118:e205–e211. <http://dx.doi.org/10.1542/peds.2005-2661>
- Fu, Y.X., and D.D. Chaplin. 1999. Development and maturation of secondary lymphoid tissues. *Annu. Rev. Immunol.* 17:399–433. <http://dx.doi.org/10.1146/annurev.immunol.17.1.399>
- Fütterer, A., K. Mink, A. Luz, M.H. Kosco-Vilbois, and K. Pfeffer. 1998. The lymphotoxin  $\beta$  receptor controls organogenesis and affinity maturation in peripheral lymphoid tissues. *Immunity.* 9:59–70. [http://dx.doi.org/10.1016/S1074-7613\(00\)80588-9](http://dx.doi.org/10.1016/S1074-7613(00)80588-9)
- Ganef, C., C. Remouchamps, L. Boutaffala, C. Bénézech, G. Galopin, S. Vandepaer, F. Bouillenne, S. Ormenese, A. Chariot, P. Schneider, et al. 2011. Induction of the alternative NF- $\kappa$ B pathway by lymphotoxin

- $\alpha\beta$  (LT $\alpha\beta$ ) relies on internalization of LT $\beta$  receptor. *Mol. Cell. Biol.* 31:4319–4334. <http://dx.doi.org/10.1128/MCB.05033-11>
- Gorbachev, A.V., and R.L. Fairchild. 2004. CD4<sup>+</sup> T cells regulate CD8<sup>+</sup> T cell-mediated cutaneous immune responses by restricting effector T cell development through a Fas ligand-dependent mechanism. *J. Immunol.* 172:2286–2295. <http://dx.doi.org/10.4049/jimmunol.172.4.2286>
- Gray, C.M., C. Remouchamps, K.A. McCorkell, L.A. Solt, E. Dejardin, J.S. Orange, and M.J. May. 2014. Noncanonical NF- $\kappa$ B signaling is limited by classical NF- $\kappa$ B activity. *Sci. Signal.* 7:ra13. <http://dx.doi.org/10.1126/scisignal.2004557>
- Hanson, E.P., L. Monaco-Shawver, L.A. Solt, L.A. Madge, P.P. Banerjee, M.J. May, and J.S. Orange. 2008. Hypomorphic nuclear factor- $\kappa$ B essential modulator mutation database and reconstitution system identifies phenotypic and immunologic diversity. *J. Allergy Clin. Immunol.* 122:1169–1177. e16. <http://dx.doi.org/10.1016/j.jaci.2008.08.018>
- Harrell, M.I., B.M. Iritani, and A. Ruddell. 2008. Lymph node mapping in the mouse. *J. Immunol. Methods.* 332:170–174. <http://dx.doi.org/10.1016/j.jim.2007.11.012>
- Hayden, M.S., and S. Ghosh. 2008. Shared principles in NF- $\kappa$ B signaling. *Cell.* 132:344–362. <http://dx.doi.org/10.1016/j.cell.2008.01.020>
- Hayden, M.S., and S. Ghosh. 2012. NF- $\kappa$ B, the first quarter-century: remarkable progress and outstanding questions. *Genes Dev.* 26:203–234. <http://dx.doi.org/10.1101/gad.183434.111>
- Hayden, M.S., A.P. West, and S. Ghosh. 2006. NF- $\kappa$ B and the immune response. *Oncogene.* 25:6758–6780. <http://dx.doi.org/10.1038/sj.onc.1209943>
- Hoffmann, A., T.H. Leung, and D. Baltimore. 2003. Genetic analysis of NF- $\kappa$ B/Rel transcription factors defines functional specificities. *EMBO J.* 22:5530–5539. <http://dx.doi.org/10.1093/emboj/cdg534>
- Imamura, M., T. Kawai, S. Okada, K. Izawa, T. Takachi, H. Iwabuchi, S. Yoshida, R. Hosokai, H. Kanegane, T. Yamamoto, et al. 2011. Disseminated BCG infection mimicking metastatic nasopharyngeal carcinoma in an immunodeficient child with a novel hypomorphic NEMO mutation. *J. Clin. Immunol.* 31:802–810. <http://dx.doi.org/10.1007/s10875-011-9568-9>
- Janssen, R., A. van Wengen, M.A. Hoeve, M. ten Dam, M. van der Burg, J. van Dongen, E. van de Vosse, M. van Tol, R. Bredius, T.H. Ottenhoff, et al. 2004. The same I $\kappa$ B $\alpha$  mutation in two related individuals leads to completely different clinical syndromes. *J. Exp. Med.* 200:559–568. <http://dx.doi.org/10.1084/jem.20040773>
- Karin, M., and Y. Ben-Neriah. 2000. Phosphorylation meets ubiquitination: the control of NF- $\kappa$ B activity. *Annu. Rev. Immunol.* 18:621–663. <http://dx.doi.org/10.1146/annurev.immunol.18.1.621>
- Kawai, T., R. Nishikomori, and T. Heike. 2012. Diagnosis and treatment in anhidrotic ectodermal dysplasia with immunodeficiency. *Allergol. Int.* 61:207–217.
- Kere, J., A.K. Srivastava, O. Montonen, J. Zonana, N. Thomas, B. Ferguson, F. Munoz, D. Morgan, A. Clarke, P. Baybayan, et al. 1996. X-linked anhidrotic (hypohidrotic) ectodermal dysplasia is caused by mutation in a novel transmembrane protein. *Nat. Genet.* 13:409–416. <http://dx.doi.org/10.1038/ng0895-409>
- Kim, D., R.E. Mebius, J.D. MacMicking, S. Jung, T. Cupedo, Y. Castellanos, J. Rho, B.R. Wong, R. Josien, N. Kim, et al. 2000. Regulation of peripheral lymph node genesis by the tumor necrosis factor family member TRANCE. *J. Exp. Med.* 192:1467–1478. <http://dx.doi.org/10.1084/jem.192.10.1467>
- Koduru, S., L. Kumar, M.J. Massaad, N. Ramesh, S. Le Bras, E. Ozcan, M.K. Oyoshi, M. Kaku, Y. Fujiwara, L. Kremer, et al. 2010. Cdc42 interacting protein 4 (CIP4) is essential for integrin-dependent T-cell trafficking. *Proc. Natl. Acad. Sci. USA.* 107:16252–16256. <http://dx.doi.org/10.1073/pnas.1002747107>
- Koike, R., T. Nishimura, R. Yasumizu, H. Tanaka, Y. Hataba, Y. Hataba, T. Watanabe, S. Miyawaki, and M. Miyasaka. 1996. The splenic marginal zone is absent in lymphoplastic aly mutant mice. *Eur. J. Immunol.* 26:669–675. <http://dx.doi.org/10.1002/eji.1830260324>
- Kong, Y.Y., H. Yoshida, I. Sarosi, H.L. Tan, E. Timms, C. Capparelli, S. Morony, A.J. Oliveira-dos-Santos, G. Van, A. Itie, et al. 1999. OPG is a key regulator of osteoclastogenesis, lymphocyte development and lymph-node organogenesis. *Nature.* 397:315–323. <http://dx.doi.org/10.1038/16852>
- Koni, P.A., R. Sacca, P. Lawton, J.L. Browning, N.H. Ruddle, and R.A. Flavell. 1997. Distinct roles in lymphoid organogenesis for lymphotoxins  $\alpha$  and  $\beta$  revealed in lymphotoxin  $\beta$ -deficient mice. *Immunity.* 6:491–500. [http://dx.doi.org/10.1016/S1074-7613\(00\)80292-7](http://dx.doi.org/10.1016/S1074-7613(00)80292-7)
- Körner, H., M. Cook, D.S. Riminton, F.A. Lemckert, R.M. Hoek, B. Ledermann, F. Köntgen, B. Fazekas de St Groth, and J.D. Sedgwick. 1997. Distinct roles for lymphotoxin- $\alpha$  and tumor necrosis factor in organogenesis and spatial organization of lymphoid tissue. *Eur. J. Immunol.* 27:2600–2609. <http://dx.doi.org/10.1002/eji.1830271020>
- Kranich, J., N.J. Krauter, E. Heinen, M. Polymenidou, C. Bridel, A. Schildknecht, C. Huber, M.H. Kosco-Vilbois, R. Zinkernagel, G. Miele, and A. Aguzzi. 2008. Follicular dendritic cells control engulfment of apoptotic bodies by secreting Mfge8. *J. Exp. Med.* 205:1293–1302. <http://dx.doi.org/10.1084/jem.20071019>
- Laurikkala, J., J. Pispá, H.S. Jung, P. Nieminen, M. Mikkola, X. Wang, U. Saarialho-Kere, J. Galceran, R. Grosschedl, and I. Thesleff. 2002. Regulation of hair follicle development by the TNF signal ectodysplasin and its receptor Edar. *Development.* 129:2541–2553.
- Liptay, S., R.M. Schmid, E.G. Nabel, and G.J. Nabel. 1994. Transcriptional regulation of NF- $\kappa$ B2: evidence for  $\kappa$ B-mediated positive and negative autoregulation. *Mol. Cell. Biol.* 14:7695–7703.
- Lo, J.C., S. Basak, E.S. James, R.S. Quiambo, M.C. Kinsella, M.L. Alegre, F. Weih, G. Franzoso, A. Hoffmann, and Y.X. Fu. 2006. Coordination between NF- $\kappa$ B family members p50 and p52 is essential for mediating LT $\beta$ R signals in the development and organization of secondary lymphoid tissues. *Blood.* 107:1048–1055. <http://dx.doi.org/10.1182/blood-2005-06-2452>
- Lopez-Granados, E., J.E. Keenan, M.C. Kinney, H. Leo, N. Jain, C.A. Ma, R. Quinones, E.W. Gelfand, and A. Jain. 2008. A novel mutation in NFKBIA/IKBA results in a degradation-resistant N-truncated protein and is associated with ectodermal dysplasia with immunodeficiency. *Hum. Mutat.* 29:861–868. <http://dx.doi.org/10.1002/humu.20740>
- Matsumoto, M., Y.X. Fu, H. Molina, G. Huang, J. Kim, D.A. Thomas, M.H. Nahm, and D.D. Chaplin. 1997. Distinct roles of lymphotoxin  $\alpha$  and the type I tumor necrosis factor (TNF) receptor in the establishment of follicular dendritic cells from non-bone marrow-derived cells. *J. Exp. Med.* 186:1997–2004. <http://dx.doi.org/10.1084/jem.186.12.1997>
- Matsushima, A., T. Kaisho, P.D. Rennert, H. Nakano, K. Kurosawa, D. Uchida, K. Takeda, S. Akira, and M. Matsumoto. 2001. Essential role of nuclear factor (NF)- $\kappa$ B-inducing kinase and inhibitor of  $\kappa$ B (I $\kappa$ B) kinase  $\alpha$  in NF- $\kappa$ B activation through lymphotoxin  $\beta$  receptor, but not through tumor necrosis factor receptor I. *J. Exp. Med.* 193:631–636. <http://dx.doi.org/10.1084/jem.193.5.631>
- McDonald, D.R., J.L. Mooster, M. Reddy, E. Bawle, E. Secord, and R.S. Geha. 2007. Heterozygous N-terminal deletion of I $\kappa$ B $\alpha$  results in functional nuclear factor  $\kappa$ B haploinsufficiency, ectodermal dysplasia, and immune deficiency. *J. Allergy Clin. Immunol.* 120:900–907. <http://dx.doi.org/10.1016/j.jaci.2007.08.035>
- Mebius, R.E. 2003. Organogenesis of lymphoid tissues. *Nat. Rev. Immunol.* 3:292–303. <http://dx.doi.org/10.1038/nri1054>
- Miyawaki, S., Y. Nakamura, H. Suzuka, M. Koba, R. Yasumizu, S. Ikehara, and Y. Shibata. 1994. A new mutation, aly, that induces a generalized lack of lymph nodes accompanied by immunodeficiency in mice. *Eur. J. Immunol.* 24:429–434. <http://dx.doi.org/10.1002/eji.1830240224>
- Napetschnig, J., and H. Wu. 2013. Molecular basis of NF- $\kappa$ B signaling. *Annu. Rev. Biophys.* 42:443–468. <http://dx.doi.org/10.1146/annurev-biophys-083012-130338>
- Ohnishi, H., R. Miyata, T. Suzuki, T. Nose, K. Kubota, Z. Kato, H. Kaneko, and N. Kondo. 2012. A rapid screening method to detect autosomal-dominant ectodermal dysplasia with immune deficiency syndrome. *J. Allergy Clin. Immunol.* 129:578–580. <http://dx.doi.org/10.1016/j.jaci.2011.09.042>
- Okamoto, N., R. Chihara, C. Shimizu, S. Nishimoto, and T. Watanabe. 2007. Artificial lymph nodes induce potent secondary immune responses in naive and immunodeficient mice. *J. Clin. Invest.* 117:997–1007. <http://dx.doi.org/10.1172/JCI130379>
- Orange, J.S., and R.S. Geha. 2003. Finding NEMO: genetic disorders of NF- $\kappa$ B activation. *J. Clin. Invest.* 112:983–985. <http://dx.doi.org/10.1172/JCI19960>

- Orange, J.S., A. Jain, Z.K. Ballas, L.C. Schneider, R.S. Geha, and F.A. Bonilla. 2004. The presentation and natural history of immunodeficiency caused by nuclear factor  $\kappa$ B essential modulator mutation. *J. Allergy Clin. Immunol.* 113:725–733. <http://dx.doi.org/10.1016/j.jaci.2004.01.762>
- Orange, J.S., O. Levy, and R.S. Geha. 2005. Human disease resulting from gene mutations that interfere with appropriate nuclear factor- $\kappa$ B activation. *Immunol. Rev.* 203:21–37. <http://dx.doi.org/10.1111/j.0105-2896.2005.00221.x>
- Pasparakis, M., L. Alexopoulou, V. Episkopou, and G. Kollias. 1996. Immune and inflammatory responses in TNF alpha-deficient mice: a critical requirement for TNF alpha in the formation of primary B cell follicles, follicular dendritic cell networks and germinal centers, and in the maturation of the humoral immune response. *J. Exp. Med.* 184:1397–1411. <http://dx.doi.org/10.1084/jem.184.4.1397>
- Pasparakis, M., L. Alexopoulou, M. Grell, K. Pfizenmaier, H. Bluethmann, and G. Kollias. 1997. Peyer's patch organogenesis is intact yet formation of B lymphocyte follicles is defective in peripheral lymphoid organs of mice deficient for tumor necrosis factor and its 55-kDa receptor. *Proc. Natl. Acad. Sci. USA.* 94:6319–6323. <http://dx.doi.org/10.1073/pnas.94.12.6319>
- Picard, C., J.L. Casanova, and A. Puel. 2011. Infectious diseases in patients with IRAK-4, MyD88, NEMO, or I $\kappa$ B $\alpha$  deficiency. *Clin. Microbiol. Rev.* 24:490–497. <http://dx.doi.org/10.1128/CMR.00001-11>
- Pillai, S., A. Cariappa, and S.T. Moran. 2005. Marginal zone B cells. *Annu. Rev. Immunol.* 23:161–196. <http://dx.doi.org/10.1146/annurev.immunol.23.021704.115728>
- Puel, A., C. Picard, C.L. Ku, A. Smahi, and J.L. Casanova. 2004. Inherited disorders of NF- $\kappa$ B-mediated immunity in man. *Curr. Opin. Immunol.* 16:34–41. <http://dx.doi.org/10.1016/j.coi.2003.11.013>
- Rajewsky, K. 1996. Clonal selection and learning in the antibody system. *Nature.* 381:751–758. <http://dx.doi.org/10.1038/381751a0>
- Rennett, P.D., J.L. Browning, R. Mebius, F. Mackay, and P.S. Hochman. 1996. Surface lymphotoxin alpha/beta complex is required for the development of peripheral lymphoid organs. *J. Exp. Med.* 184:1999–2006. <http://dx.doi.org/10.1084/jem.184.5.1999>
- Rennett, P.D., P.S. Hochman, R.A. Flavell, D.D. Chaplin, S. Jayaraman, J.L. Browning, and Y.X. Fu. 2001. Essential role of lymph nodes in contact hypersensitivity revealed in lymphotoxin- $\alpha$ -deficient mice. *J. Exp. Med.* 193:1227–1238. <http://dx.doi.org/10.1084/jem.193.11.1227>
- Roosendaal, R., and R.E. Mebius. 2011. Stromal cell-immune cell interactions. *Annu. Rev. Immunol.* 29:23–43. <http://dx.doi.org/10.1146/annurev-immunol-031210-101357>
- Schimke, L.F., N. Rieber, S. Rylaarsdam, O. Cabral-Marques, N. Hubbard, A. Puel, L. Kallmann, S.A. Sombke, G. Notheis, H.P. Schwarz, et al. 2013. A novel gain-of-function *IKBA* mutation underlies ectodermal dysplasia with immunodeficiency and polyendocrinopathy. *J. Clin. Immunol.* 33:1088–1099. <http://dx.doi.org/10.1007/s10875-013-9906-1>
- Seymour, R., J.P. Sundberg, and H. Hogensch. 2006. Abnormal lymphoid organ development in immunodeficient mutant mice. *Vet. Pathol.* 43:401–423. <http://dx.doi.org/10.1354/vp.43-4-401>
- Shih, V.F., R. Tsui, A. Caldwell, and A. Hoffmann. 2011. A single NF $\kappa$ B system for both canonical and non-canonical signaling. *Cell Res.* 21:86–102. <http://dx.doi.org/10.1038/cr.2010.161>
- Shinkura, R., K. Kitada, F. Matsuda, K. Tashiro, K. Ikuta, M. Suzuki, K. Kogishi, T. Serikawa, and T. Honjo. 1999. A lymphoplasia is caused by a point mutation in the mouse gene encoding NF- $\kappa$ B-inducing kinase. *Nat. Genet.* 22:74–77. <http://dx.doi.org/10.1038/8780>
- Shultz, D.B., M.R. Rani, J.D. Fuller, R.M. Ransohoff, and G.R. Stark. 2009. Roles of IKK- $\beta$ , IRF1, and p65 in the activation of chemokine genes by interferon- $\gamma$ . *J. Interferon Cytokine Res.* 29:817–824. <http://dx.doi.org/10.1089/jir.2009.0034>
- Snapper, C.M., P. Zelazowski, F.R. Rosas, M.R. Kehry, M. Tian, D. Baltimore, and W.C. Sha. 1996. B cells from p50/NF- $\kappa$ B knock-out mice have selective defects in proliferation, differentiation, germ-line CH transcription, and Ig class switching. *J. Immunol.* 156:183–191.
- Srivastava, A.K., M.C. Durmowicz, A.J. Hartung, J. Hudson, L.V. Ouzts, D.M. Donovan, C.Y. Cui, and D. Schlessinger. 2001. Ectodysplasin-A1 is sufficient to rescue both hair growth and sweat glands in Tabby mice. *Hum. Mol. Genet.* 10:2973–2981. <http://dx.doi.org/10.1093/hmg/10.26.2973>
- Tsitsikov, E.N., J.C. Gutierrez-Ramos, and R.S. Geha. 1997. Impaired CD19 expression and signaling, enhanced antibody response to type II T independent antigen and reduction of B-1 cells in CD81-deficient mice. *Proc. Natl. Acad. Sci. USA.* 94:10844–10849. <http://dx.doi.org/10.1073/pnas.94.20.10844>
- Tucker, E., K. O'Donnell, M. Fuchsberger, A.A. Hilton, D. Metcalf, K. Greig, N.A. Sims, J.M. Quinn, W.S. Alexander, D.J. Hilton, et al. 2007. A novel mutation in the *Nfkb2* gene generates an NF- $\kappa$ B2 “super repressor”. *J. Immunol.* 179:7514–7522. <http://dx.doi.org/10.4049/jimmunol.179.11.7514>
- Tumanov, A.V., S.I. Grivennikov, A.N. Shakhov, S.A. Rybtsov, E.P. Koroleva, J. Takeda, S.A. Nedospasov, and D.V. Kuprash. 2003. Dissecting the role of lymphotoxin in lymphoid organs by conditional targeting. *Immunol. Rev.* 195:106–116. <http://dx.doi.org/10.1034/j.1600-065X.2003.00071.x>
- van de Pavert, S.A., and R.E. Mebius. 2010. New insights into the development of lymphoid tissues. *Nat. Rev. Immunol.* 10:664–674. <http://dx.doi.org/10.1038/nri2832>
- van de Pavert, S.A., B.J. Olivier, G. Goverse, M.F. Vondenhoff, M. Greuter, P. Beke, K. Kusser, U.E. Höpken, M. Lipp, K. Niederreither, et al. 2009. Chemokine CXCL13 is essential for lymph node initiation and is induced by retinoic acid and neuronal stimulation. *Nat. Immunol.* 10:1193–1199. <http://dx.doi.org/10.1038/ni.1789>
- Vondenhoff, M.F., M. Greuter, G. Goverse, D. Elewaut, P. Dewint, C.F. Ware, K. Hoorweg, G. Kraal, and R.E. Mebius. 2009. LT $\beta$ R signaling induces cytokine expression and up-regulates lymphangiogenic factors in lymph node anlagen. *J. Immunol.* 182:5439–5445. <http://dx.doi.org/10.4049/jimmunol.0801165>
- Wang, B., H. Fujisawa, L. Zhuang, I. Freed, B.G. Howell, S. Shahid, G.M. Shivji, T.W. Mak, and D.N. Sauder. 2000. CD4<sup>+</sup> Th1 and CD8<sup>+</sup> type 1 cytotoxic T cells both play a crucial role in the full development of contact hypersensitivity. *J. Immunol.* 165:6783–6790. <http://dx.doi.org/10.4049/jimmunol.165.12.6783>
- Ware, C.F., T.L. VanArsdale, P.D. Crowe, and J.L. Browning. 1995. The ligands and receptors of the lymphotoxin system. *Curr. Top. Microbiol. Immunol.* 198:175–218.
- Weih, F., D. Carrasco, S.K. Durham, D.S. Barton, C.A. Rizzo, R.P. Ryseck, S.A. Lira, and R. Bravo. 1995. Multiorgan inflammation and hematopoietic abnormalities in mice with a targeted disruption of RelB, a member of the NF- $\kappa$ B/Rel family. *Cell.* 80:331–340. [http://dx.doi.org/10.1016/0092-8674\(95\)90416-6](http://dx.doi.org/10.1016/0092-8674(95)90416-6)
- Weih, D.S., Z.B. Yilmaz, and F. Weih. 2001. Essential role of RelB in germinal center and marginal zone formation and proper expression of homing chemokines. *J. Immunol.* 167:1909–1919. <http://dx.doi.org/10.4049/jimmunol.167.4.1909>
- Winning, S., F. Spletstoesser, J. Fandrey, and S. Frede. 2010. Acute hypoxia induces HIF-independent monocyte adhesion to endothelial cells through increased intercellular adhesion molecule-1 expression: the role of hypoxic inhibition of prolyl hydroxylase activity for the induction of NF- $\kappa$ B. *J. Immunol.* 185:1786–1793. <http://dx.doi.org/10.4049/jimmunol.0903244>
- Xu, J. 2005. Preparation, culture, and immortalization of mouse embryonic fibroblasts. *Curr. Protoc. Mol. Biol.* Chapter 28:Unit 28.1. <http://dx.doi.org/10.1002/0471142727.mb2801s70>
- Yoshioka, T., R. Nishikomori, J. Hara, K. Okada, Y. Hashii, I. Okafuji, S. Nodomi, T. Kawai, K. Izawa, H. Ohnishi, et al. 2013. Autosomal dominant anhidrotic ectodermal dysplasia with immunodeficiency caused by a novel NFKBIA mutation, p.Ser36Tyr, presents with mild ectodermal dysplasia and non-infectious systemic inflammation. *J. Clin. Immunol.* 33:1165–1174. <http://dx.doi.org/10.1007/s10875-013-9924-z>